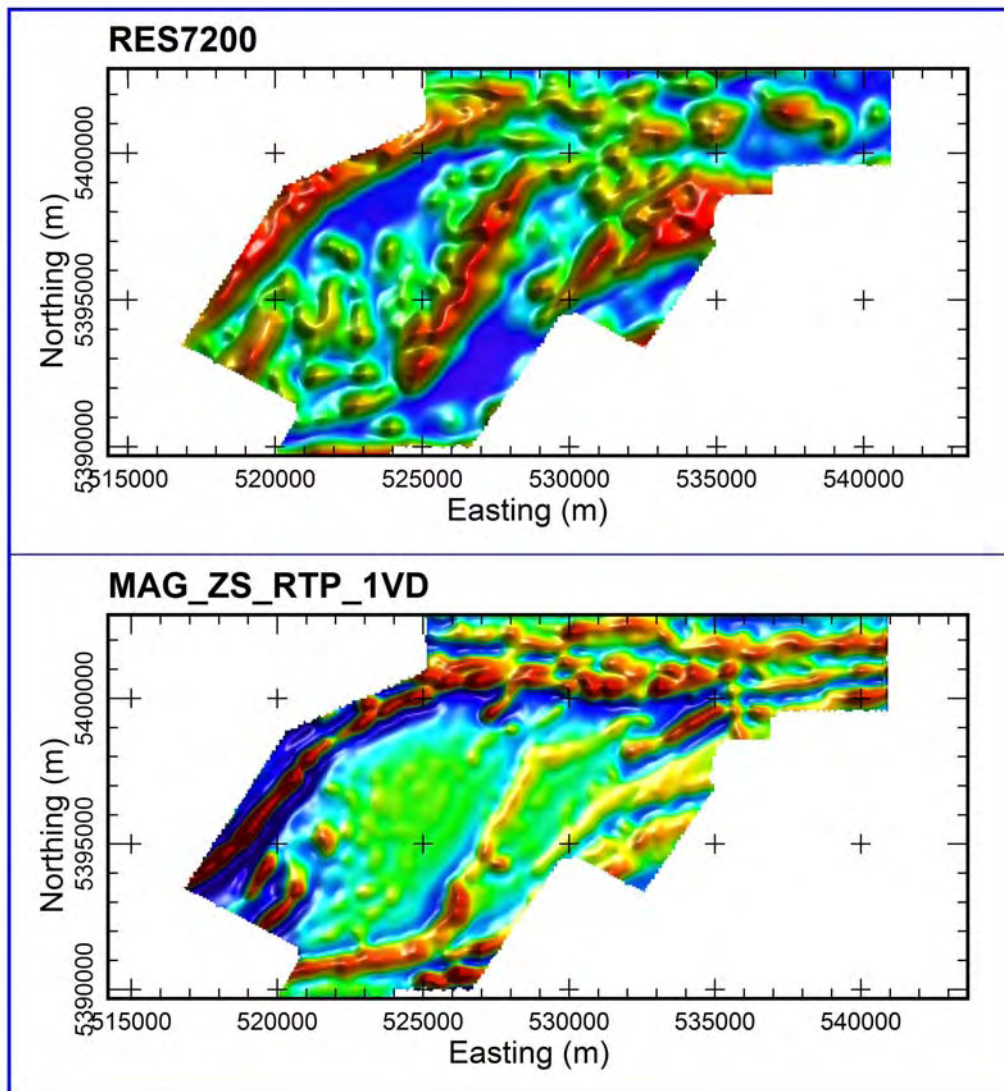# REPORT ON PROCESSING AND ANALYSIS

OF A DIGHEM EM & MAGNETIC SURVEY

MINE CENTRE/BAD VERMILION LAKE PROPERTY

FORT FRANCES AREA, ONTARIO

Q-GOLD RESOURCES LTD.

OCTOBER 2006

Condor Consulting
Lakewood Colorado
USA

Condor Consulting, Inc.

REPORT ON PROCESSING AND ANALYSIS

OF A DIGHEM EM & MAGNETIC SURVEY

MINE CENTRE/BAD VERMILION LAKE PROPERTY

FORT FRANCES AREA, ONTARIO

Q-GOLD RESOURCES LTD.

OCTOBER 2006

Condor Consulting
Lakewood Colorado
USA

CONTENTS

1. SUMMARY

This report covers the processing and analysis of Dighem frequency-domain EM and magnetic surveys carried out for Q-Gold (Ontario) Ltd. (Q-Gold) on their Mine Centre/Bad Vermilion Lake project areas, located near Fort Frances, Ontario. The purpose of the survey was to assist in the location of gold mineralization. An INPUT EM and magnetic data set complemented the geophysical data available for interpretation.

The EM data were examined for anomalies that might indicate zones of gold mineralization. Several anomalies were located that are felt to warrant additional follow-up. The lack of more anomalous responses is attributed to two factors; the dominate modes of mineralization are gold within quartz veins and gold associated with disseminated sulfides; neither of these modes of occurrence are expected to shown strong EM responses. In addition, the presence of conductive clays associated with lakes and the drainage has likely masked any subtle underlying EM sources.

In addition to assessing the EM results, a basic structural assessment was made of the magnetic data; this has provided additional targets for follow-up.

In terms of ground follow-up, the IP-resistivity technique is recommended as this would be well suited to mapping the dominant style of mineralization on the property.

2. INTRODUCTION

Fugro Airborne Survey Corp. (Fugro) undertook a Dighem helicopter EM and magnetic survey over the Mine Centre/ Bad Vermilion Lake project area in May 2006. A total of 1,516 lkm were flown in three blocks. Details of the work are provided in Garrie (2006). The general locations of the survey are shown below in Figures 1-3.
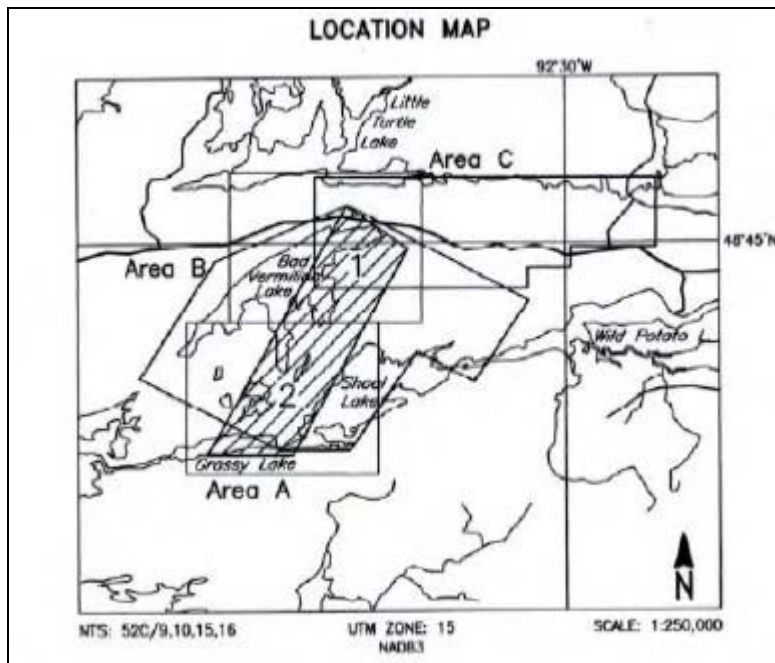

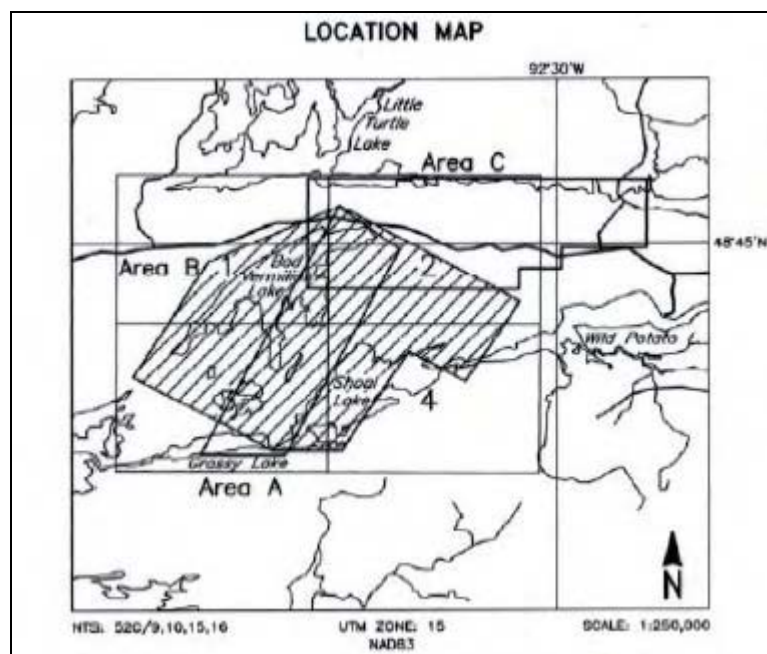Figure 1: Location of Survey Area A

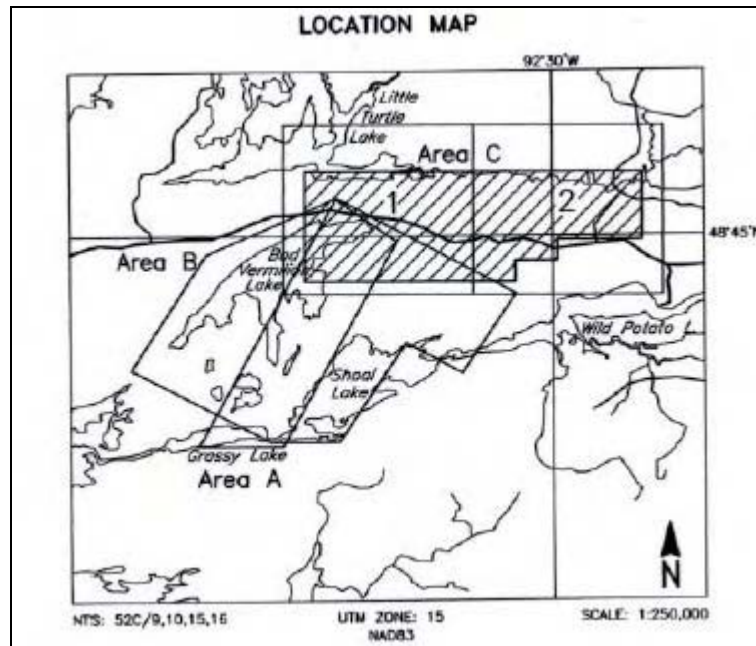
Figure 2: Location of Survey Area B.

Figure 3: Location of Survey Area C

The area was also covered by INPUT data acquired in an airborne survey in 1980 at a line spacing of 200 m (OGS 2003).

Condor Consulting, Inc. (Condor) was commissioned by Q-Gold in September 2006 to undertake an assessment of survey results. Q-Gold provided the Fugro report and data bases, a geological base map and vector files of the drainage and infrastructure (railroad, roads, utility pipes). In addition, Q-Gold provided Condor with a short geological discussion of the area and the location of five (5) Focus Areas; this material is included in Appendix A. Condor acquired the INPUT survey direct from the Ontario Geological Survey.

3. LOCAL GEOLOGY AND TARGET MODELS

The study area was reviewed by Poulsen (1983) and the following description of the local geology was provided (reference is provided in Appendix A).

Laminated, gold-bearing quartz veins in the Mine Centre - Fort Frances area occur in ductile shear zones and as dilations of regionally developed cleavage. These structures are related kinematically to large transcurrent faults in the region. Gold mineralization is thought to be entirely epigenetic and possibly related to seismic pumping of fluids during faulting. A similar spatial relationship between gold and large fault zones exists throughout the

Wabigoon Subprovince and recognition of related subsidiary structures should be one objective of an exploration strategy for gold in this region.
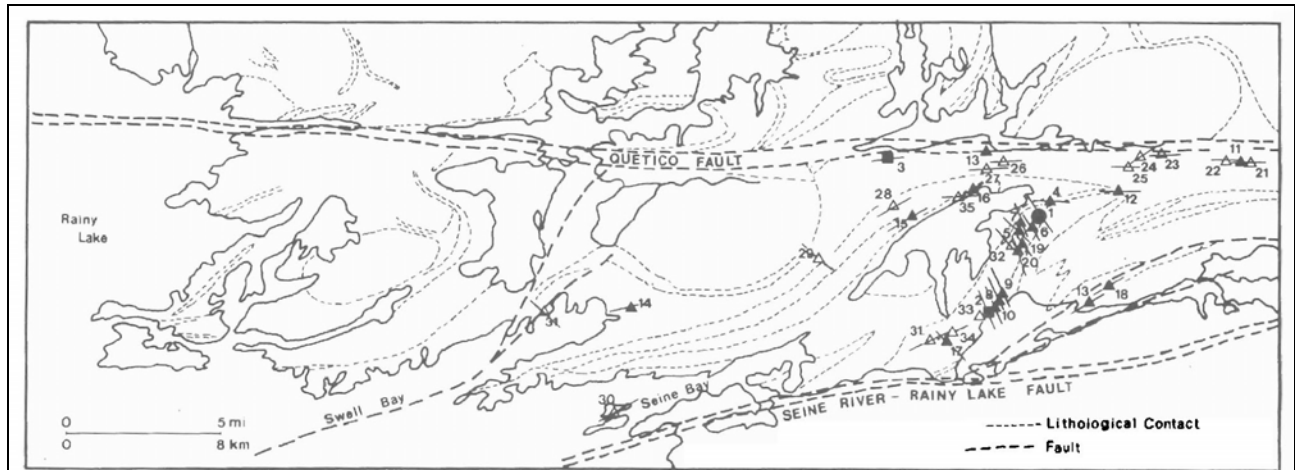
Figure 4: Regional geologic map of study area (after Poulsen 1983)

At the property scale Bolen (2006) notes that the gold mineralization occurs in a preserved wedge of greenstone rocks between the E-W trending Rainy Lake-Seine River Fault on the south and the Quetico Fault on the north. Locally within the greenstone wedge, the relative movement of the two major fault zones (with the Quetico Fault moving westward relative to Rainy Lake-Seine River Fault) has created a series of sigmoidal dilation zones into which a series of gold-bearing felsic intrusive rocks have been emplaced in a number of secondary fault structures.

The geological structures at a variety of scales can also be expected to show expression in the magnetic data. At the property scale, the overall outline of a complete dilation zone is well captured in the magnetic data as shown in Figure 5.
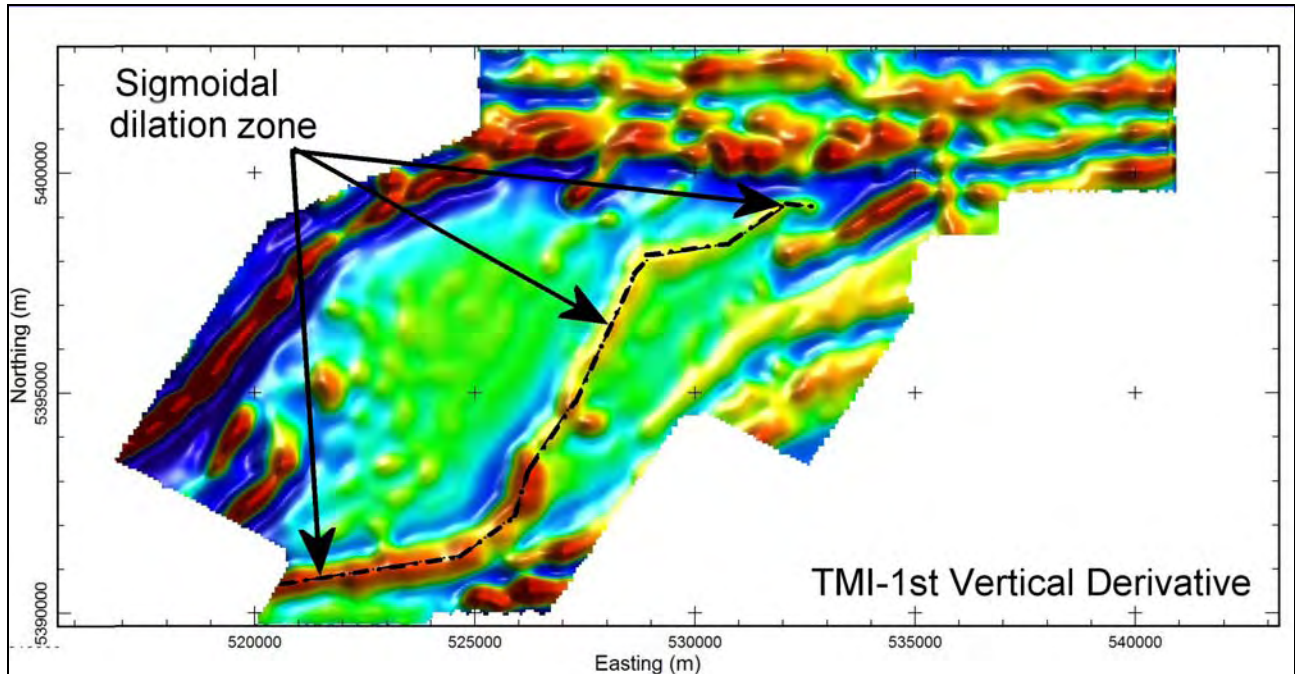
Figure 5: Example of sigmoidal dilation zone expressed in magnetic data

In terms of the expected geophysical response at the deposit scale, there appears to be two dominant modes of occurrence; gold-bearing zones associated with quartz veins and gold with disseminated conductive minerals such as chalcopyrite, pyrite and pyrrhotite. For the former situation, a resistivity high could be expected and for the later, a moderate conductor.

4. PROCESSING, ANALYSIS TECHNIQUES AND PRODUCTS

PROCESSING

Stitching and Microleveling

While no microleveling of the EM data was required, the three Dighem magnetic grids were stitched and leveled. The INPUT magnetic data was then merged with the final Dighem magnetic grid.

Layered-earth Inversion (FarEM)

FarEM is a product of the University of British Colombia, Geophysical Inversion Facility (Farquharson and Oldenburg, 2000). The program (informally referred to historically as EM1dFM) is a layered earth inversion (LEI) routine designed to model frequency domain EM of the variety typically recorded with Max-Min (ground) or Dighem-style helicopter EM systems. The program can recover both conductivity and magnetic permeability of the subsurface within the limits of the specific acquisition system being employed. The benefit of this processing is that the perturbation to the EM data caused by the magnetic permeability is removed, thereby providing for a 'clean' EM signal for subsequent processing. In the current assessment, the recovered magnetic permeability information was not used in the interpretation.

FarEM Processing Parameters

All five EM components (three co-planar & two coaxial) were used in the inversion. A total of 28 logarithmically spaced layers, ranging from 1 m to 26.5 m were used, to a maximum depth of 250 m.

Starting conductivity: 0.0001 S/m (10,000 Ω-m)
Reference conductivity: 0.0001 S/m (10,000 Ω-m)
Fixed Trade-off with Beta: 2

FarEM Plotting Parameters

Conductivities are in the form of conductivity depth sections (CDS) and are presented in units of ohm-m and are plotted with a color bar range of 10 - 5,000 Ω-m for both surveys. Additional information on CDS processing is provided in Appendix B.

Time Constant-Tau

Time constants (taus) were derived from the Dighem data using proprietary software developed by EMSolutions LLC. The algorithm derives time constants from the in-phase and quadrature responses

at two frequencies making use of the definition of decay currents in frequency-domain as described by Macnae et al. (1998). Since the impact of noise and magnetic permeability effects is strongest on low-frequency responses, best results were obtained from the EM responses at the two highest frequencies (56 kHz and 7,200 Hz). The tau grids and profiles shown in this report were derived from the 7.2/56 kHz data.

Time Constant-AdTau

The AdTau program calculates the time constant (tau) from time domain decay data. The program is termed **_AdTau_** since rather than using a fixed suite of channels as commonly done, the user sets a noise level and depending on the local characteristics of the data, the program will then select the set of five channels above this noise level. In resistive areas, the earlier channels will tend to be used, whereas in conductive terrains the latest channels available can generally be used. A typical decay fit; in this case, the last five channels are shown to the right in Figure 6. AdTau processing was applied to the INPUT EM data. Further details on AdTau are provided in Appendix C.
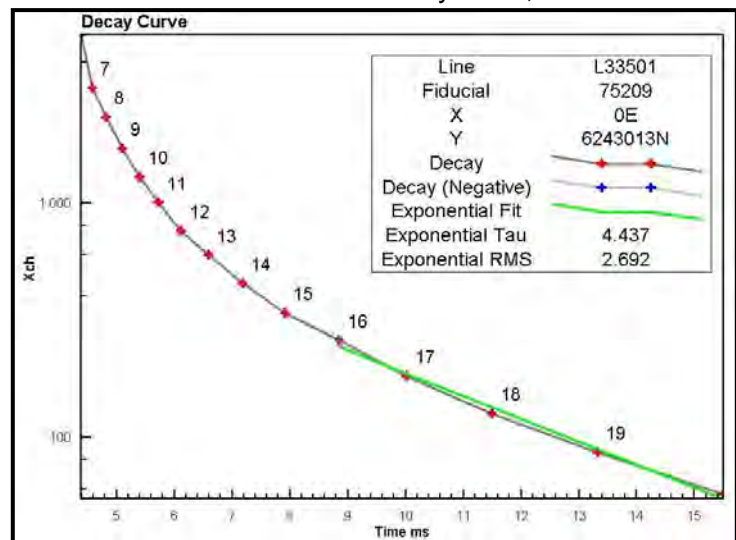

Figure 6: Typical decay curve

ZS Filtering of Magnetic Data

The ZS suite of filtered magnetic results was produced using Profile Analyst[1]. The ZS filtering suite is one of a new class of derivative-based may be used to improve the precision of source edge detection and, by extension, the determination of the spatial extent of magnetic units. These filters are demonstrated to perform successfully on both strongly magnetized features as well as on weakly magnetized or deep magnetic features. The software and algorithms are described by Shi and Butt (2004) – this paper is included in Appendix D

---

[1] Profile Analyst is a product of Encom Technology Ltd.

Discrete Body Modeling

Discrete body modeling of several magnetic features of interest south and east of the Foley Mine was undertaken. This work was done using the Encom Model Vision Pro and QuickMag applications. See Appendix E for details.

ANALYSIS TECHNIQUES

EM Picking

The MultiPlot™ display was the primary means to identify and rank the anomalies. This overall process is termed anomaly picking and was done on a line-by-line basis, with several passes being required to finalize the process.

An EM picking scheme was used that made use of the following data:
- EM profiles
- Time-constant (Tau and AdTau) profiles and grids
- Conductivity-depth sections
- Power line monitor
- Drainage, lake, power line, utility and road vector files
- Geology

The picking data bases generated by Condor are provided in Excel and Geosoft formats on the archival DVD.

Discrete Features

Discrete features are considered to be those EM responses which are interpreted to be caused by conductors with limited lateral dimensions.

Wide Zones

There were numerous broad zones of conductive character noted in the results, mostly related to lake sediments and drainage channels; these were designated as Wide Zones (WZs). The WZs were not themselves considered targets per se but were identified and indexed as part of the overall characterization of the conductivity environment.

Target Zones

Groupings of conductors are termed Target Zones or TZ. A TZ is deemed as a logical grouping of conductors within the data set and is based on an assessment of the distribution of individual conductor picks, plus any other available geoscience data. The TZs are then prioritized for follow up work based on their overall geophysical character.

Ranking of EM Picks

A ranking scheme, using the following anomaly classification was used:

Rank 0 - cultural source, such as power line, road, utility.

Rank 1 - excellent; strong low-frequency response.

Rank 2 - low-medium; could be related to cultural source or overburden

Rank 3 - surficial; most likely related to drainage

Rank 4 - surficial; coincide with mapped lakes/drainage

All WZs fall within classifications 3 and 4. Examples of the ranking features are shown in Figures 7a and 7b; designated as Picking MultiPlots™. Note these vary slightly with the final MultiPlots™ as described in tabulated products in Table 4-1.

MAGNETICS

The magnetic assessment was done using a variety of the products; including the TMI, 1VD and the ZS suite. Rather than selecting discrete picks, a series of Target Zones were identified based on an assessment of lineations inferred to be structurally related. Apart from selection of the Target Zones, no further ranking of these Target Zones was undertaken.
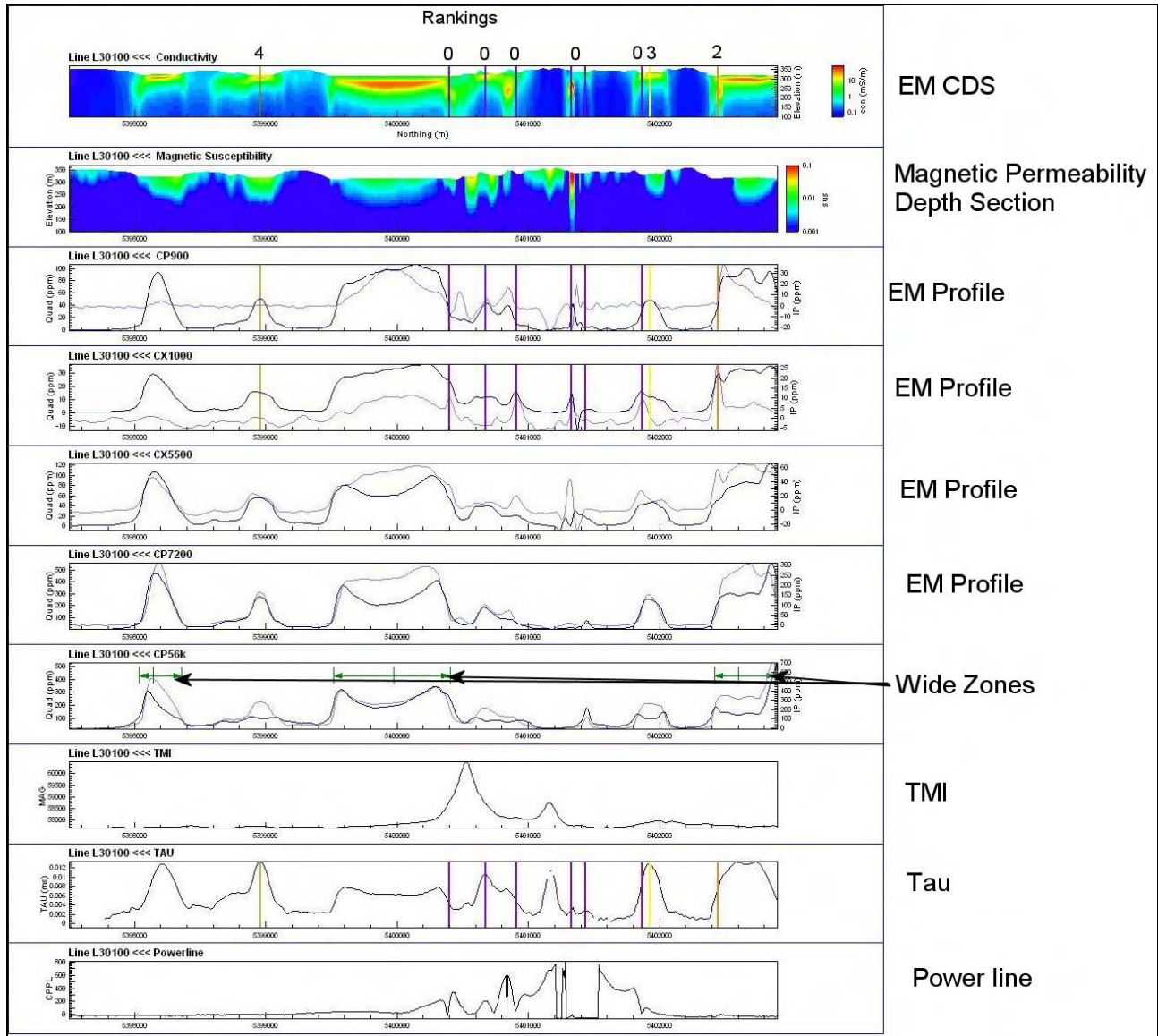
Figure 7a: Picking MultiPlots with ranked anomalies for L30100. Wide Zones are indicated in green in the CP56k panel.
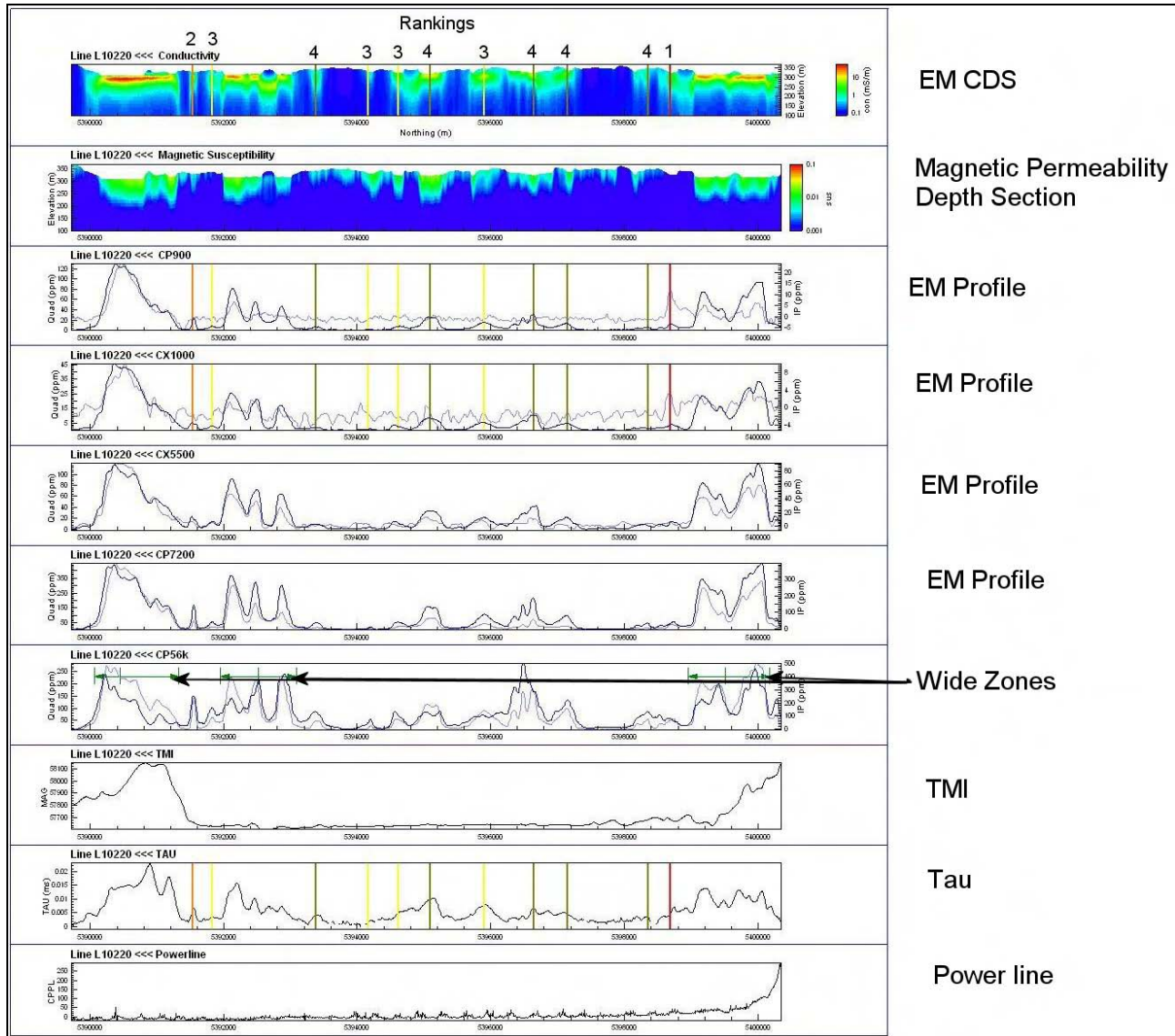
Figure 7b: Picking MultiPlots with ranked anomalies for L10220. Wide Zones are indicated in green in the CP56k panel.

PRODUCTS

Table 4-1 lists the maps and products that are provided. Other products can be prepared from the existing dataset, if required.

Base Maps-All maps are created using the following parameters:

<u>Projection Description</u>:

Datum:	NAD 83
Ellipsoid:	GRS80
Projection:	UTM (Zone: 15N)
Central Meridian:	93ºW
False Northing:	0
False Easting:	500,000
Scale Factor:	0.9996
WGS84 to Local Conversion:	Molodensky

Table 4-1 Survey Products

<u>TargetMaps</u> @ 1:20,000 (one copy of each)

Maps include the Condor Picks EM + Wide Zones + Mag Target Zones + interpreted magnetic lineaments + Q-Gold Focus areas

- TMI
- 1st Vertical Derivative of TMI
- Tau (derived from Dighem EM data)
- DTM with Apparent resistivity-56 kHz contours
- Geology
- Geology + Dighem + INPUT EM picks (from contractor's data bases)
- Overburden thickness map derived from EM results
- ZS Magnetic Filtering Suite

<u>MultiPlots</u>™ @ 1:20,000 (digital only)

Mini-Plates™: TMI, 1st Vertical Derivative of TMI, Tau, Geology and DTM

On each MultiPlot™ the Condor picks are indicated along with the following:

- Profile 1: Coplanar In-phase and Quadrature: 56,000 Hz, 7,200 Hz, and 900 Hz
- Profile 2: Coaxial In-phase and Quadrature: 5,500 Hz and 1,000 Hz
- Profile 3: Total magnetic intensity (TMI), 1st Vertical Derivative of TMI, power line monitor
- Profile 4: Tau, Apparent Resistivity 56,000 Hz, 7,200 Hz and 900 Hz
- CDS with EM system height + Wide Zones

- TrackMap 1: 1st Vertical Derivative of TMI + flight path + magnetic Target Zones

- TrackMap 2: Tau + flight path + EM picks

- TrackMap 3: Geology + flight path + EM picks + Focus Areas

Survey Report (1 copy)

On the archive DVD the following files are provided:

-Digital XYZ archive in Geosoft format

-Digital grid archives in Geosoft format

-Anomaly data bases in Excel and Geosoft formats

-PDFs of TargetMaps and MultiPlots™

-Survey report (PDF)

5. SURVEY RESULTS

GENERAL

The regional geological setting and geophysical deposit models for the study are discussed in Section 3; a resistivity high associated with gold in quartz veins and a moderate conductivity high associated with gold hosted in disseminated sulfides. For neither model was the geophysical response regarded as particularly diagnostic in light of the 1) extensive areas of high resistivity associated with areas of topographic relief and extensive areas of low resistivity associated with lake sediments, swamps and cultural responses.

EM and Magnetic Outcomes

Figures 8-14 summarize the outcomes of the EM and magnetic interpretation. The EM and magnetic anomaly picks are displayed on the Dighem flight path (Figure 8), the drainage (Figure 9), geology (Figure 10), total magnetic intensity (Figure 11), first vertical derivative of the TMI (Figure 12), time constant (Figure 13) and topography (Figure 14). The Focus Zones as provided by Q-Gold are also outlined on these figures.

A broad data swath in the northern area is contaminated by cultural responses due to a railway and utility line. Figure 9 shows the lakes and drainage along with picked wide zones and anomalies of all categories. It demonstrates that most of the EM data are dominated by lake sediments and other surficial clays. Only one Rank-1 target has been picked from the EM data. The other target anomalies are weak and might be related to cultural responses and/or overburden edges.

Figure 15 shows an image of the time constant derived from the INPUT data with the anomaly picks. It indicates that the strong Rank 1 EM anomaly detected in the Dighem data also shows up in the INPUT data.
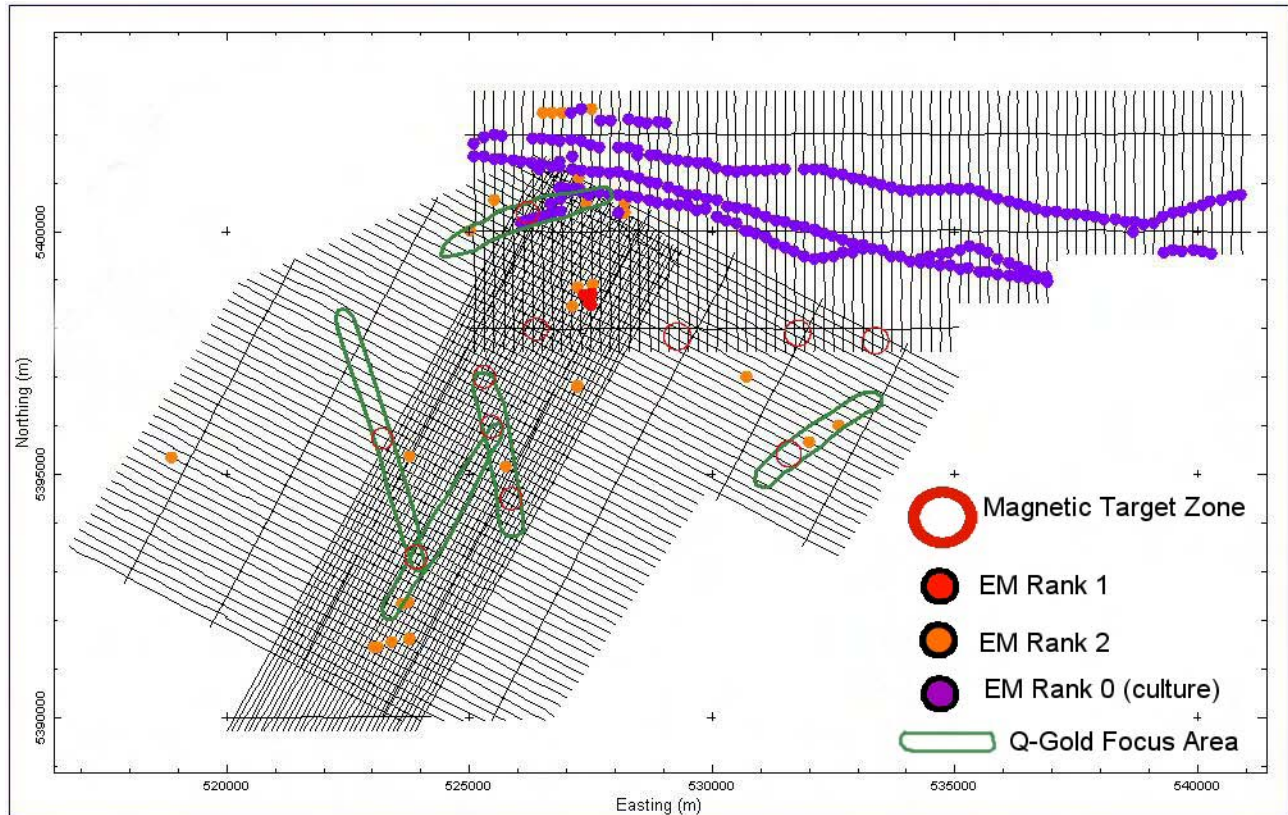
Figure 8: Flight path with EM anomaly picks (Ranking 0-2), magnetic TZs and Focus Areas
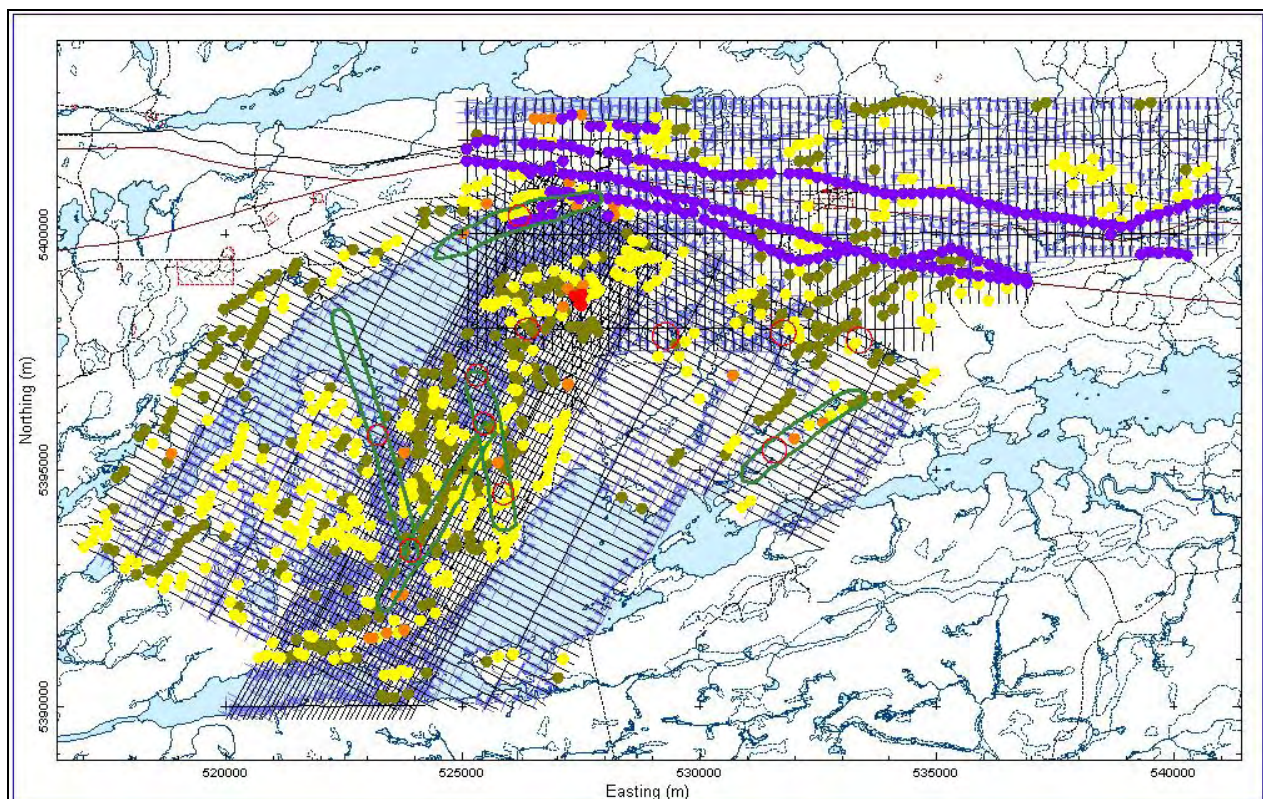

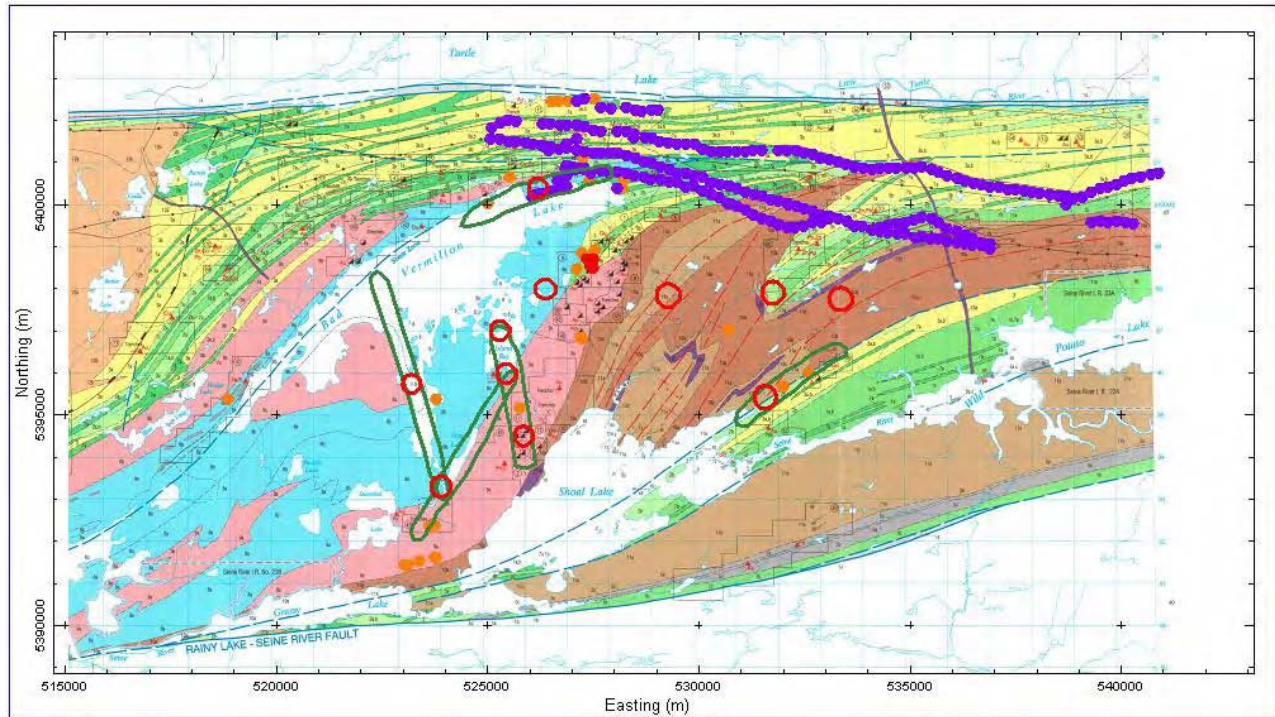Figure 9: Flight path with EM anomaly picks (Ranking 0-4), WZs and magnetic TZs on drainage.

Figure 10: Geology with EM anomaly picks (Ranking 0-2), magnetic TZs and Focus Areas

Figure 11: TMI grid with EM anomaly picks (Ranking 0-2), magnetic TZs and Focus Areas

Figure 12: 1VD grid with EM anomaly picks (Ranking 0-2), magnetic TZs and Focus Areas
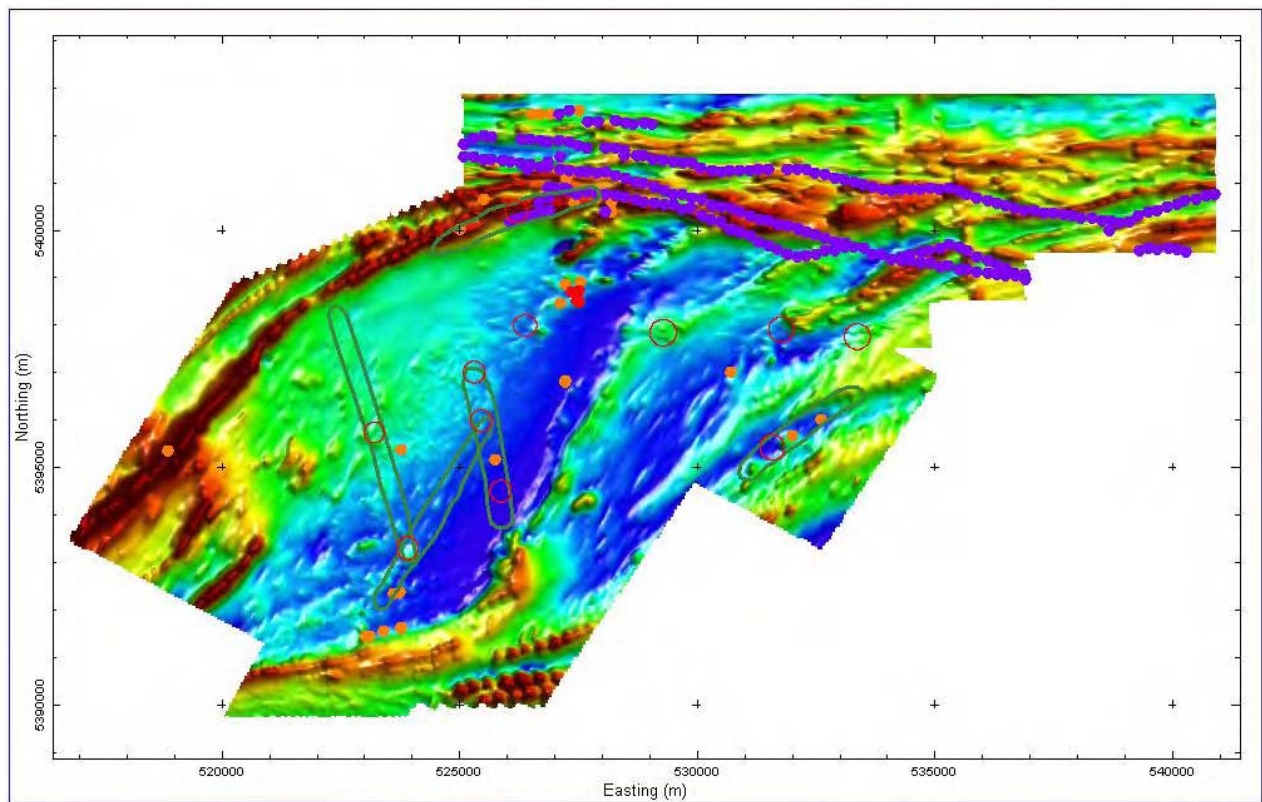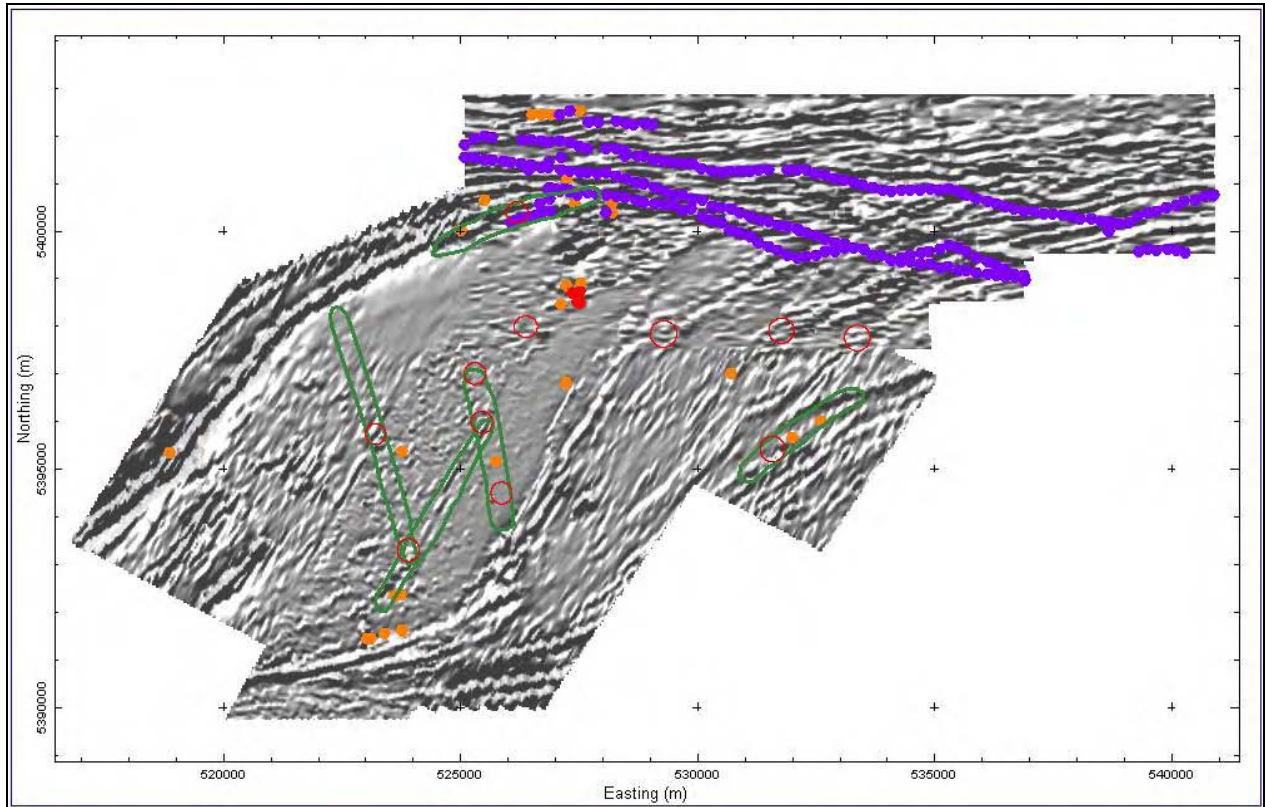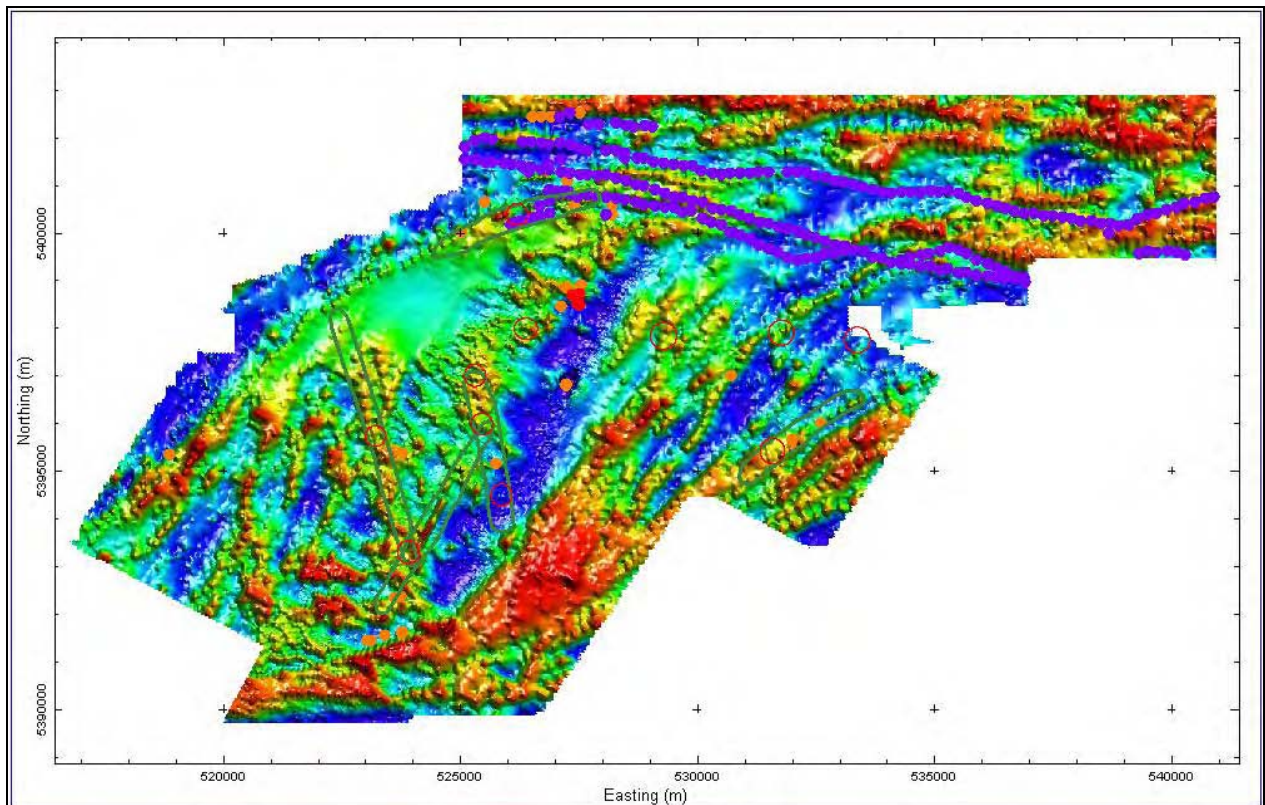

Figure 13: Tau grid with EM anomaly picks (Ranking 0-2), magnetic TZs and Focus Areas
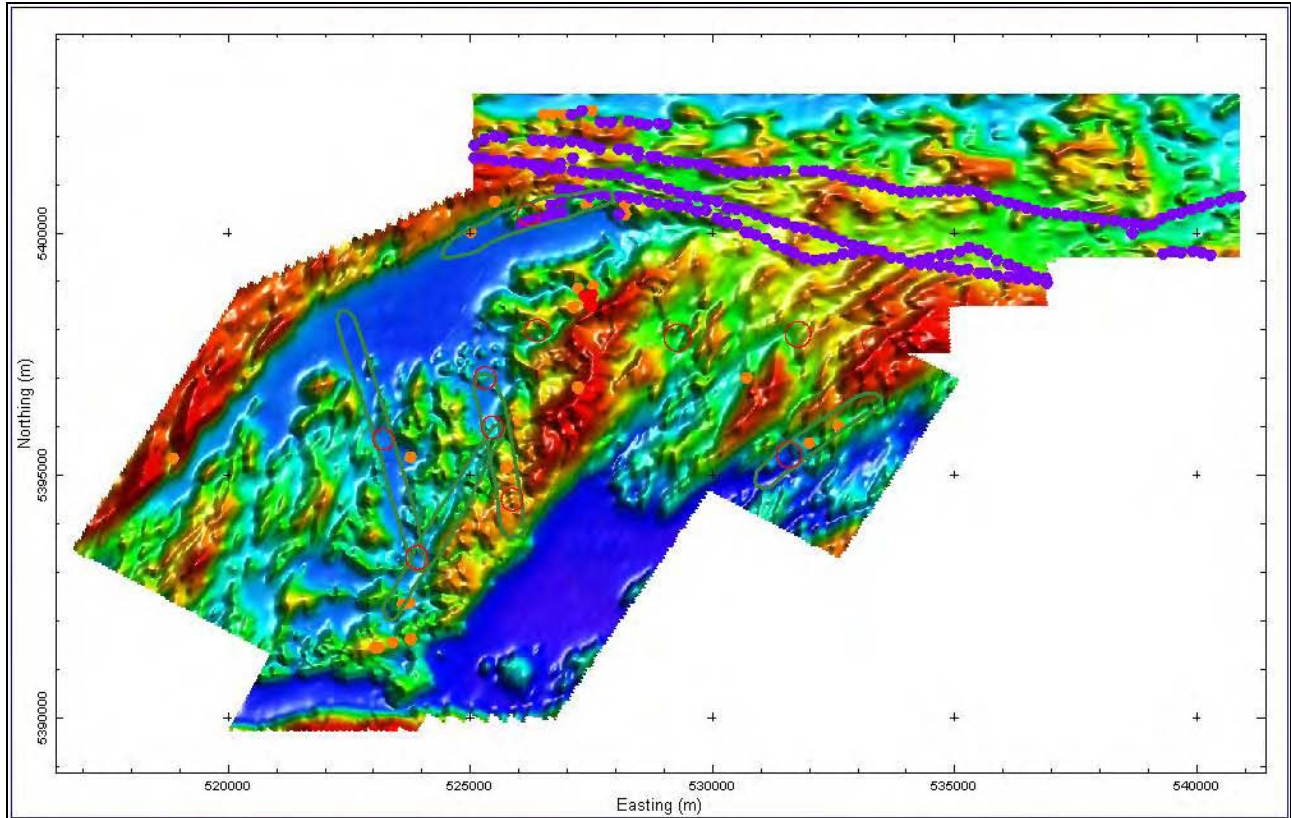
Figure 14: DTM grid with EM anomaly picks (Ranking 0-2), magnetic TZs and Focus Areas
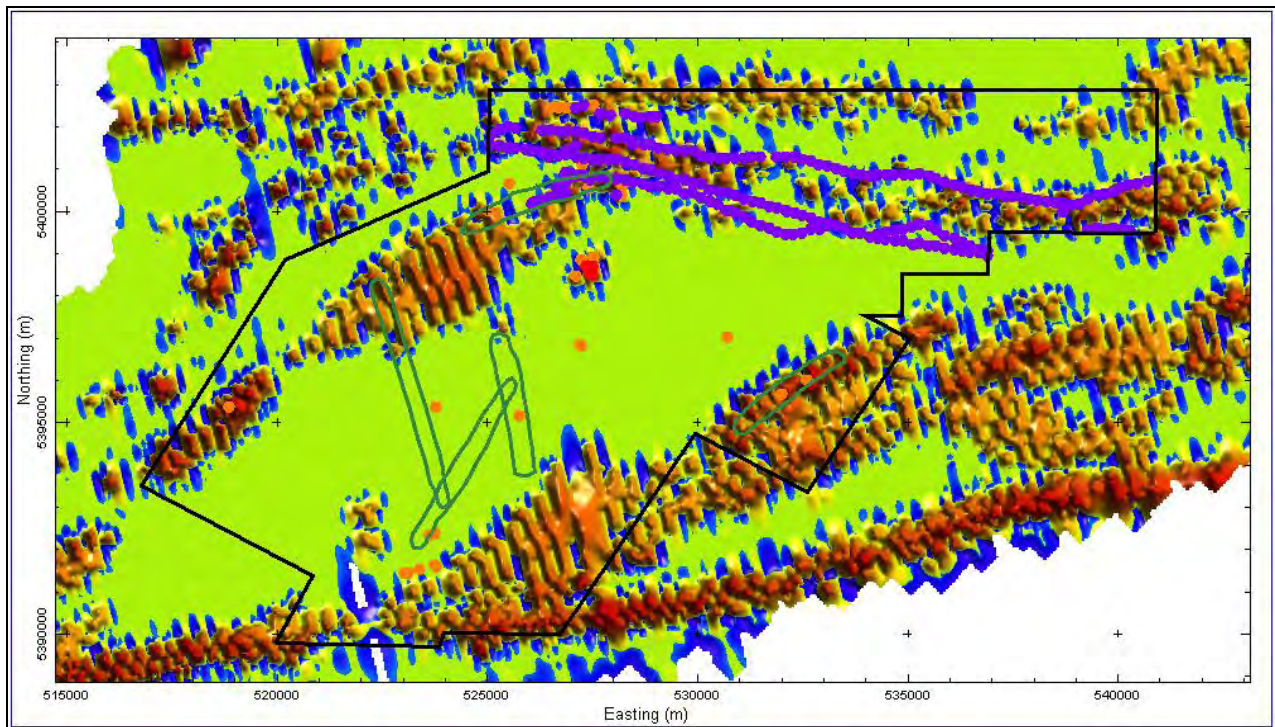

Figure 15: INPUT AdTau grid with EM anomaly picks (Ranking 0-2), magnetic TZs and Focus Areas

The Rank 1 and Rank 2 EM anomalies were grouped into Target Zones as shown in Figure 16 and listed in Table 5-1. The confidence in these target zones decreases with increasing Target Zone number.
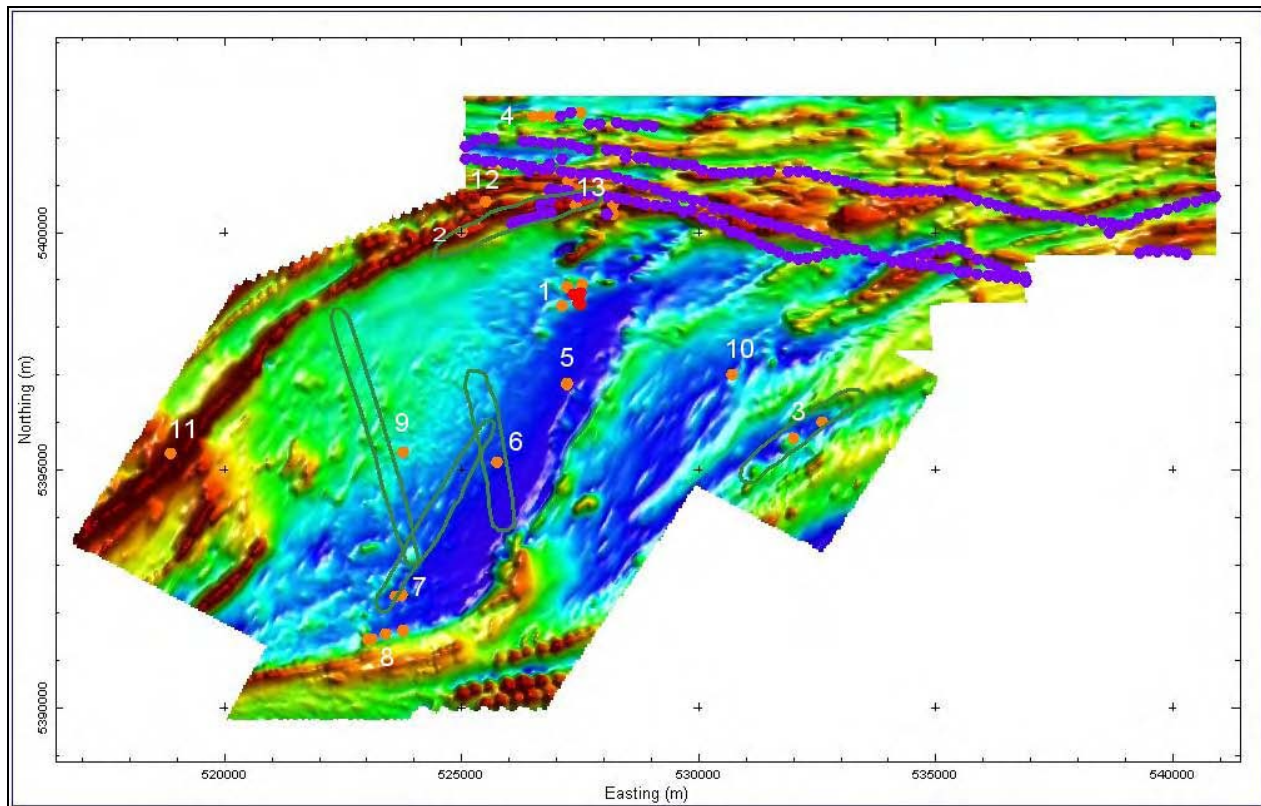
Figure 16: TMI grid with EM anomaly picks (Ranking 0-2), magnetic TZs and Focus Areas

Table 5-1: EM Target Zones.

Target Zone	ID	Line	Fid	x	y	Ranking	Comment
1	164	L10220	3191	527371.9	5398695	1	
1	180	L10230	4005	527482.5	5398658	1	
1	185	L10241	4512	527515.4	5398485	1	
1	330	L20100	3991	527545.7	5398910	2	
1	339	L20110	4411	527246.4	5398846	2	clay?
1	340	L20110	4420	527511.1	5398708	1	
1	347	L20120	4930	527462.3	5398508	1	
1	352	L20130	5228	527120.4	5398456	2	
1	718	L30130	2186	527490.7	5398503	1	
1	719	L30130	2191	527504.3	5398664	1	
2	336	L20110	4339	525007.7	5400022	2	
3	343	L20110	4599	532626.2	5396009	2	culture/clay?
3	357	L20140	6225	532019.7	5395663	2	culture/clay?
4	683	L30080	3533	526519.3	5402451	2	culture?
4	694	L30090	3372	526705.7	5402442	2	culture?
4	695	L30100	2874	526906.4	5402444	2	culture?

4	1087	L30130	2316	527529.8	5402523	2	culture?
5	242	L10300	426	527241.1	5396807	2	culture?
5	384	L20200	3358	527225.9	5396830	2	culture?
6	189	L10250	4737	525761.9	5395155	2	clay?
7	154	L10200	2616	523124.3	5391452	2	culture?
7	155	L10210	2815	523755.3	5392365	2	culture?
8	138	L10190	1953	523027.8	5391444	2	culture?
8	153	L10200	2591	523625.6	5392349	2	culture?
8	174	L10220	3416	523403.8	5391539	2	culture?
8	188	L10250	4614	523790.7	5391602	2	culture?
8	604	L20510	5567	523773.5	5391623	2	culture?
9	1068	T29030	7781	523781.9	5395380	2	edge/culture?
10	341	L20110	4531	530721.7	5397012	2	edge?
11	576	L20461	952	518882.1	5395356	2	mag artifact?
12	315	L20070	2406	525528.2	5400660	2	culture?
13	262	L20010	744	527267	5401093	2	culture?
13	265	L20010	785	528219.2	5400583	2	culture?
13	278	L20020	526	528199.4	5400379	2	culture?
13	1053	T19010	5056	527420.2	5400571	2	culture?

In order to detect zones of silicification, the EM data were examined for zones of high resistivity (or low Tau). This examination indicated a very close relationship between resistivity and topography. This is illustrated in Figure 17, which shows apparent resistivity contours from the 56,000 Hz response overlain on the topography grid. The two data sets show a very high degree of correlation and thereby confirm the earlier observation, that the EM data are dominated by the response due to the drainage system.
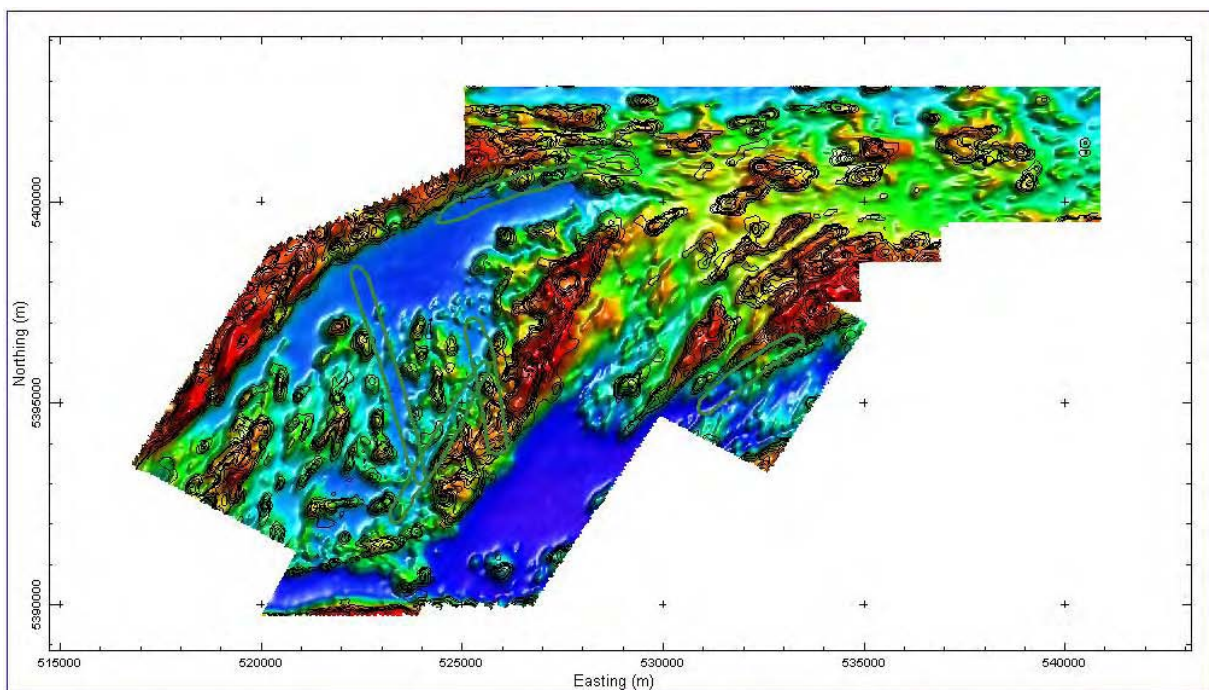

Figure 17: 56,000 Hz apparent resistivity contours on DTM grid and Focus Areas

An overburden thickness map was derived from the LEI results. For this calculation, any surficial material more conductive than 2 mS/m (500 ohm-m) was considered to be overburden.
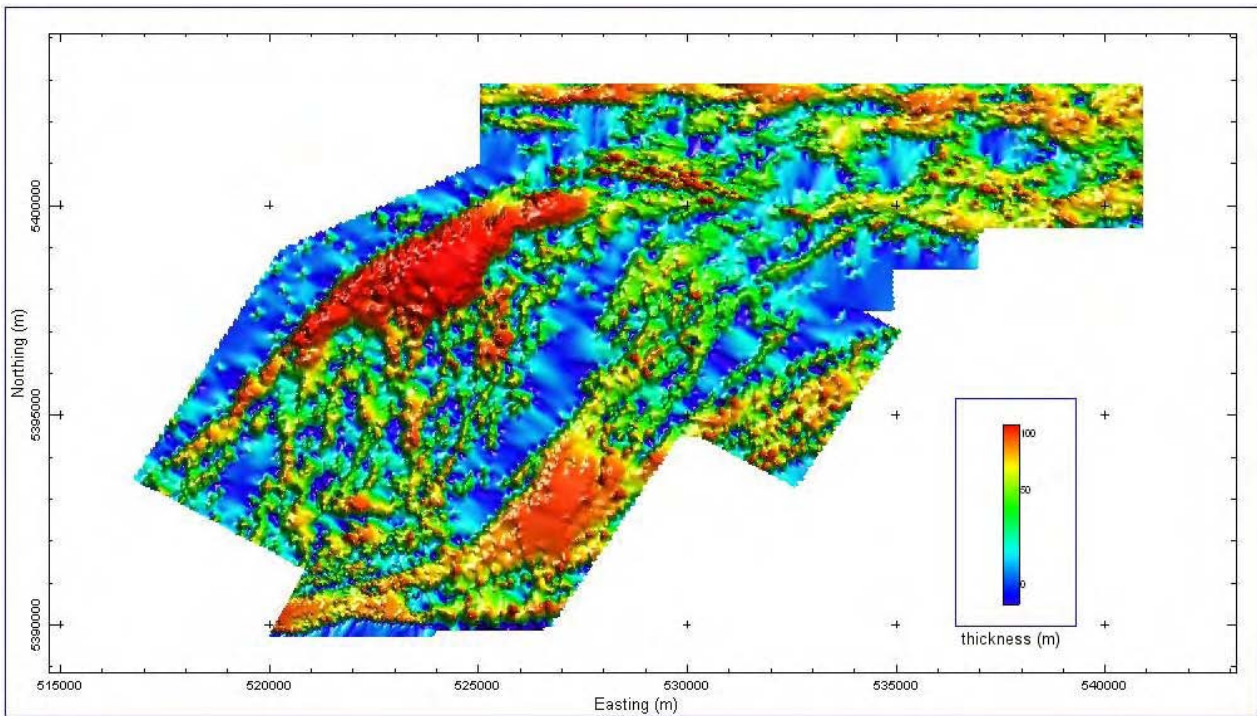

Figure 18: Overburden thickness derived from Dighem EM data.

Magnetics

The complete magnetic interpretation showing picked lineaments and TZs is summarized in Figures 19 and 20, with the TZs listed in Table 5-2. The primary criteria for selecting the TZs was the intersection of several lineaments.

Table 5-2: Magnetic Targets

X	Y
523205	5395750
523897.4	5393268
525282.3	5396976
525859.3	5394509
525441	5395966
526191.1	5400409
531543.1	5395432
526364.3	5397986
529278.3	5397856
531774	5397914
533375.2	5397741

Discrete Body Modeling

Several magnetic anomalies located south and southeast of the Foley Mine were modeled for source geometry; these are located in Figure 21. There is an outcrop of mapped lamprophyre which correlates with the northern end of the Anomaly A. While Anomaly B lies totally under water, it is also assumed to be lamprophyre.

Anomaly A: The northern part of this body was modeled using Model Vision Pro. A composite of the results are presented in Figure 22 with the full suite of modeled lines provided in Appendix E. The model shows the anomaly to be caused by a series of SE dipping plate-like sources that generally lie within 100 m depth from the surface.

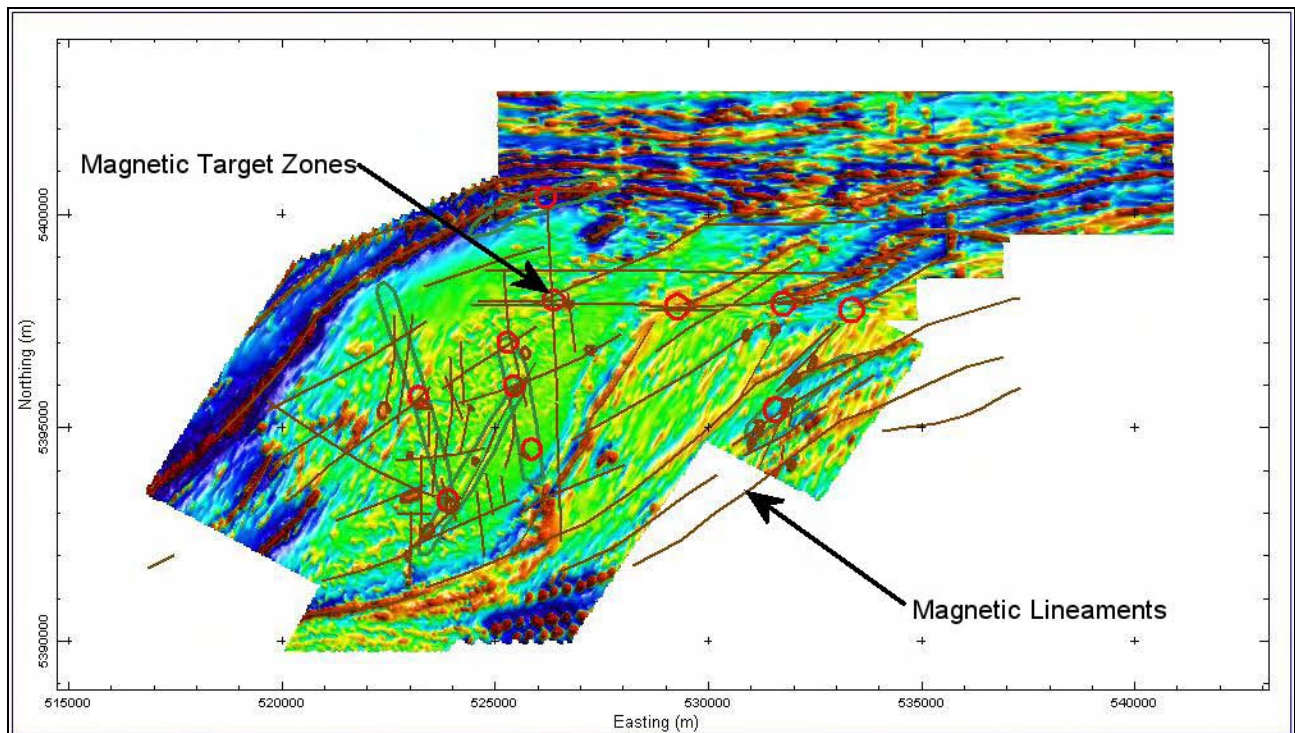Figure 19: 1VD grid with magnetic interpretation (lineaments in brown and targets in red).
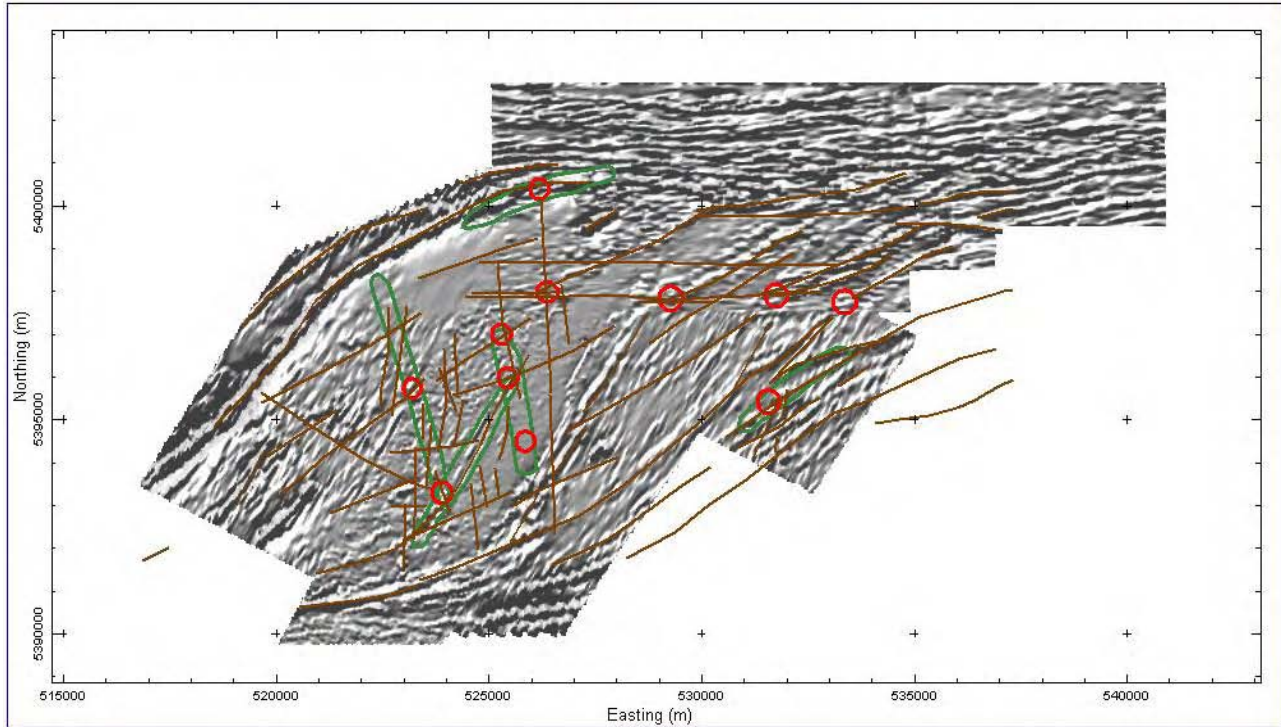
Figure 20: 1VD grid with magnetic interpretation (lineaments in brown and targets in red).

Anomaly B: This source modeled as compact shallow source (<25 m depth) dipping steeply to the north (Figure 23).
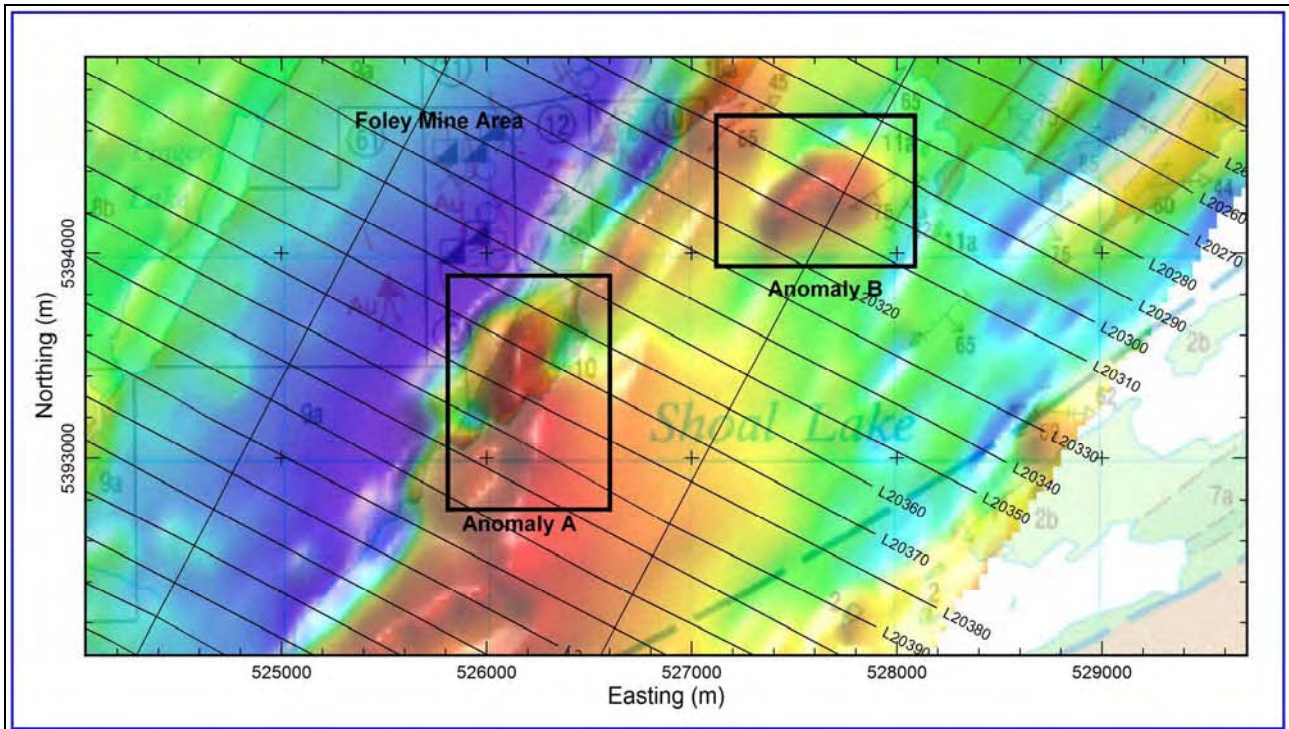

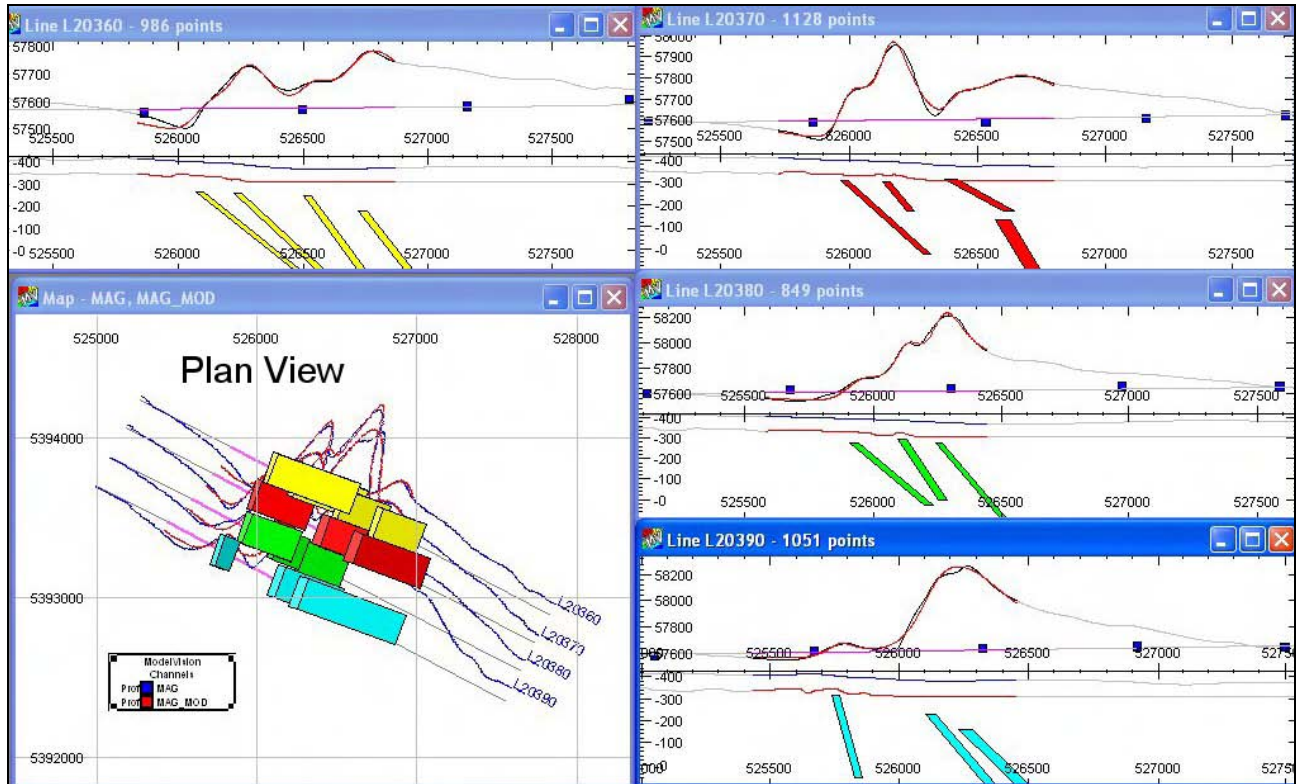Figure 21: Magnetic Features near Foley Mine Selected for modeling

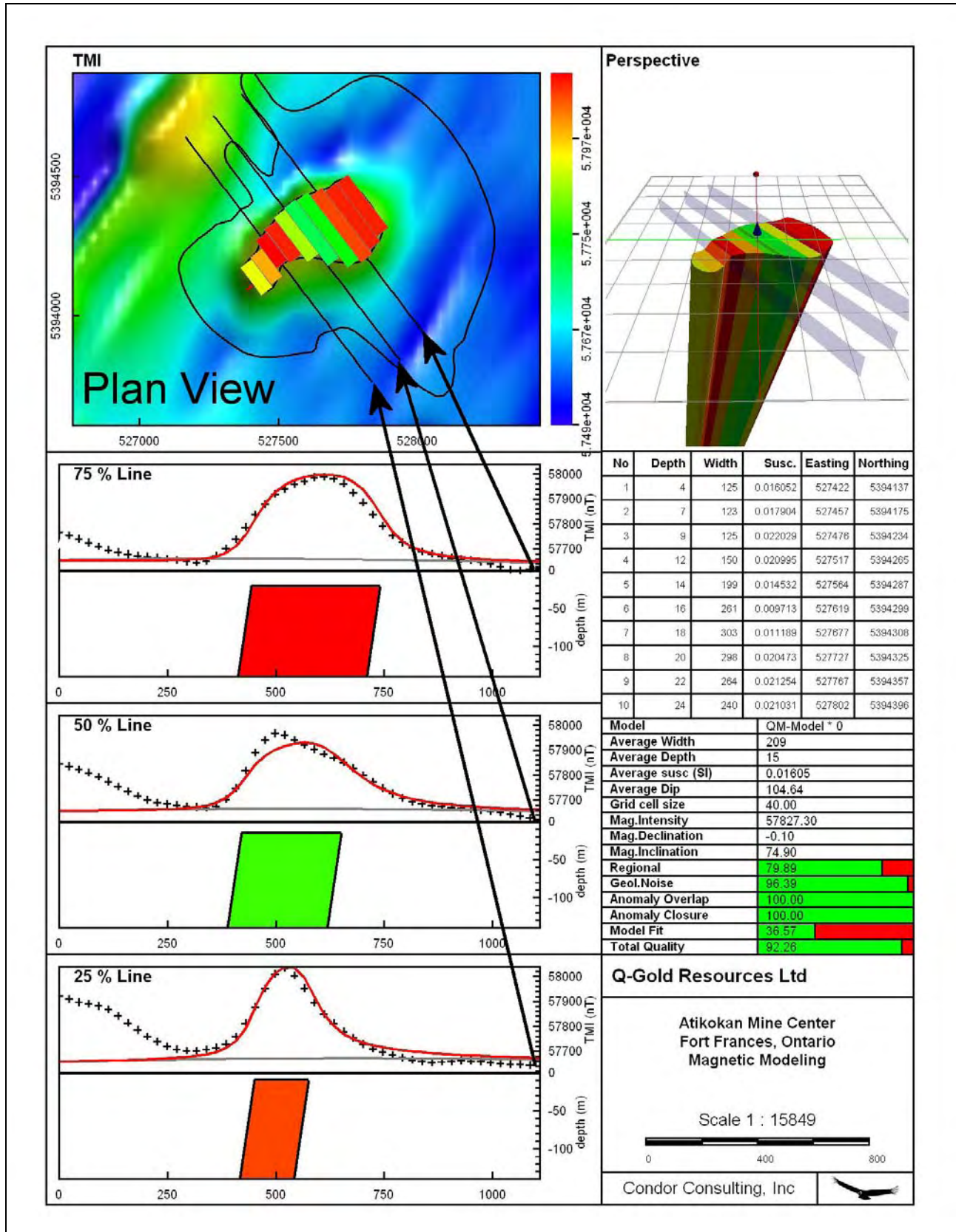Figure 22: Model Vision Pro model for Anomaly A

Figure 23: QuickMag model for Anomaly B

6. CONCLUSIONS AND RECOMMENDATIONS

This report provides a description of the processing and analysis undertaken on a Dighem EM and magnetic survey near Fort Frances, Ontario. Based on the current understanding of the dominant gold deposit models; either zones of high resistivity or moderate conductivity (discussed in Section 3), the EM technique alone was not expected to provide a well-constrained outcome. To supplement the EM results, analysis of the magnetic data was undertaken to help identify promising areas for follow-up.

In terms of outcomes, one strong Rank 1 EM anomaly was selected. All picked Rank 2 anomalies are weak and might be related to culture and/or to overburden edges. Alternatively, these expressions could be the subtle response of a gold-bearing system. The Target Zones picked from the magnetic lineament analysis provide an alternate set of features for follow-up that are dominantly structure related; earlier geological work by Poulsen (1983 and 2000) has emphasized the importance of structure in localizing gold in the study area.

Ground follow-up of either the EM anomalies or magnetic Target Zones is felt to be best done with the IP-resistivity technique. This technique will provide good sensitivity to both zones of high resistivity or moderate conductivity. The technique will also enable a greater depth of investigation than has been achieved for the Dighem survey.

Respectfully submitted,

CONDOR CONSULTING, Inc.

October 31, 2006

7. REFERENCES

Bolen, J., (2006) Personal communication

Farquharson, C. G., & Oldenburg, D. W., (2000), Automatic estimation of the trade-off parameter in nonlinear inverse problems using the GCV and L-curve criteria: SEG 70th Annual Meeting, Calgary, Alberta, 6-11 August 2000

Garrie, D., (2006) Dighem Survey for Q-Gold (Ontario) Ltd. Mine Centre/Bad Vermilion Lake: Blocks A, B & C. Fort Frances, Ontario, Canada; report number # 06040; Report by Fugro Airborne Surveys, August 2006

Macnae, J., King, A., Stolz, N., Osmakoff, A., and Blaha, A., (1998), Fast AEM data processing and inversion: Exploration Geophysics 29, 163-169.

Ontario Geological Survey 2003. Ontario airborne geophysical surveys, magnetic data, Atikokan-Mine Centre area; Ontario Geological Survey, Geophysical Data Set 1029.

Poulsen, K. H., (1983) Structural setting of vein-type gold mineralization in the Mine Centre-Fort Frances Area: Implications for the Wabigoon Subprovince; in the Geology of Gold in Ontario, edited by A. C. Colvine, Ontario Geological Survey, Miscellaneous Paper 110, 278p.

Poulsen, K. H., (2000) Precambrian geology and mineral occurrences, Mine Centre-Fort Frances area; Ontario Geological Survey, Map 2525, scale 1:50,000

Shi, Z. and Butt, G. (2004): New enhancement filters for geological mapping. ASEG 17th Geophysical Conference and Exhibition, Sydney 2004. Extended abstract.

8. APPENDIXES

APPENDIX A GEOLOGICAL REFERENCES

Q-Gold (Ontario) Ltd.

Areas of Greatest Interest:
Jack Bolen-September 29, 2006

Area 1

Along the Finger Lake Fault. At the south end of area outlined there are several zones of quartz veining with pyrite up to 30% as irregular masses with good gold grades. Magnetics should be watched closely as Lamprophyre sills are known to exist lying conformable to the NE strike of the shear zone. The Finger Lake Fault mainly follows the contact between the Anorthosite and the Trondhjemite. At the south end of Finger Lake a cross cutting shear strikes NW. The intersection point is most interesting. The Finger Lake Fault is believed to be Left Lateral in movement. This zone of intense shearing is up to 500 metres wide. The intersection point with zone 2 may be a structural trap with silicification and or sulphidization.

Area 2

NE trending cross cutting shear. The sense of movement is not known although it is probable left lateral. The 1980 airborne survey shows a weak anomaly on the tie line. Sulphide mineralization and silicification is expected. The intersection point with Area 1 and the West Bad Vermilion Fault zones are of primary interest.

Area 3

Part of the Bad Vermilion West Fault Zone. Movement is Left Lateral. The Fault primarily lays within Bad Vermilion Lake. Where the Fault Zone comes ashore on the north part of the lake numerous zones of quartz veining with high Au values have been found. The Gabbro in places has been completely replaced by silica in zones up to 20 metres width with high gold values. The volcanics to the north and south typically have up to 5% pyrite and up to 10% magnetite. The silicified zone and the gabbro is typically devoid of magnetite.

Area 4

An area of cross cutting shears. Within the Trondhjemite numerous Au bearing quartz veins exist including the Foley Mine Site. Within Island Bay 2 conductors have been outlined with a TDEM Survey and Max Min. The conductors strike basically N – S. Island Bay has a water depth that does not exceed 10 metres. The conductors are believed to be within the Gabbro/Anorthosite. A copper showing with Au is to the south on strike.; it is hosted within a 10 metre wide shear and contains 10 to 15% sulphides mainly as chalcopyrite, py and po.

Area 5

A strong Shear zone lays on the contact between Rhyolite which have been altered to sericite schist with strong chlorite alteration. This unit has very little mineralization and may be quite resistant. The north contact is with sediments, sandstones, siltstones and conglomerate (boulders with a chlorite sand matrix). The area of the shear is marked by an area up to 150 metres wide with low topo, with swamp and beaver dams. The unit to the south dips south at 70 to 80 degrees. This is the north limb of and overturned fold.

Humus sampling of the low ground returned highly anomalous Au. Silicification and or sulphidization is likely.

Hopefully this will be helpful.

Jack Bolen
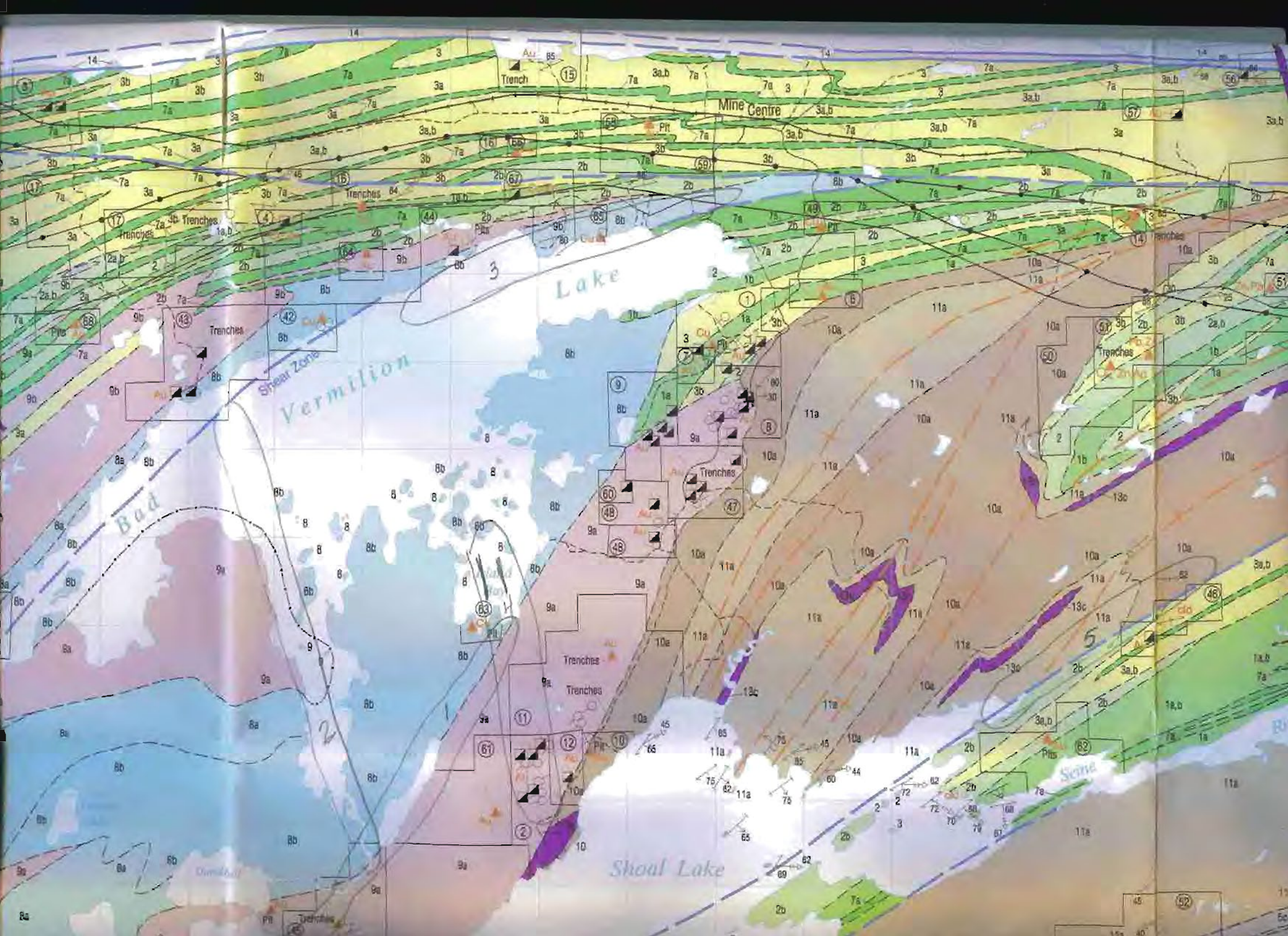
Structural Setting of Vein-Type Gold Mineralization in the Mine Centre – Fort Frances Area: Implications for the Wabigoon Subprovince

K. Howard Poulsen

Department of Geological Sciences, Queen's University, Kingston

ABSTRACT

Laminated, gold-bearing quartz veins in the Mine Centre – Fort Frances area occur in ductile shear zones and as dilations of regionally developed cleavage. These structures are related kinematically to large transcurrent faults in the region. Gold mineralization is thought to be entirely epigenetic and possibly related to seismic pumping of fluids during faulting. A similar spatial relationship between gold and large fault zones exists throughout the Wabigoon Subprovince and recognition of related subsidiary structures should be one objective of an exploration strategy for gold in this region.

INTRODUCTION

Early in this century, geologists were particularly aware of structural controls on vein-type gold deposits. Recent emphasis on the stratigraphic setting of Archean lode gold deposits has resulted in little application of advances in the field of structural geology to this particular problem. Specifically, a variety of structural styles involving diapir folds and shear zones have been documented in the Archean of southwestern Superior Province (Schwerdtner *et al.* 1979; Poulsen *et al.* 1980; Park 1981; Blackburn *et al.* 1982; Borradaile 1982). In all cases, a relative structural chronology has been documented and, where gold-bearing veins can be related to a particular structural episode, they too will be governed by the same chronology. Recognition of the structural association of lode gold deposits not only may provide one component of an exploration strategy for gold but also will be of value in evaluating genetic concepts for this class of deposit. The specific example of gold mineralization which occurs in the Mine Centre – Fort Frances area and the general example of the distribution of lode gold in the Wabigoon Subprovince illustrates this point.
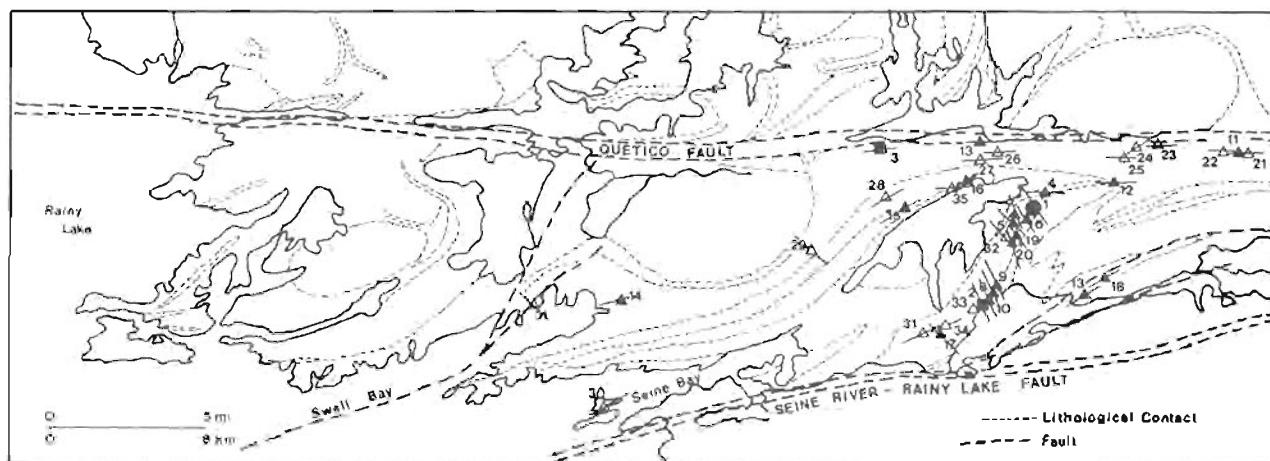
MINE CENTRE – FORT FRANCES AREA

All significant occurrences of base and precious metal mineralization in the Mine Centre – Fort Frances area lie within a wedge shaped fault block along the southwestern margin of the Wabigoon Subprovince. The northern boundary of this block is the mylonite zone comprising the Quetico Fault and the southern margin is marked by the Seine River – Rainy Lake Fault, a phyllonitic schist zone (Figure 1). Internal faults divide the block into individual domains with distinctive structural, stratigraphic and metamorphic characteristics. Two fundamental types of domain are present. To the north and west of Swell Bay (Figure 1) mafic and ultramafic metavolcanics with intercalated gabbroic sills, turbiditic metasediments and iron formations comprise the volcanic sequence which is cut by granodioritic intrusions. The rocks are metamorphosed to assemblages characteristic of the lower to upper amphibolite facies and are folded into antiforms and synforms which do not reflect the stratigraphic order. To the south and east of Swell Bay, the domains are dominated by felsic and intermediate metavolcanic compositions. Subvolcanic sills include gabbro, anorthosite, tonalite and trondhjemite and the volcanic and plutonic rocks are overlain with angular unconformity by conglomerate and arenites of probable alluvial-fluvial sedimentary facies (Wood 1980; Blackburn *et al.* 1982). The rocks in these domains form steeply dipping northward- and southward-facing panels with northeastward strike; steeply dipping cleavage is ubiquitous and greenschist facies metamorphic assemblages predominate.

STRUCTURAL SETTING OF GOLD

Gold-bearing quartz-carbonate veins have been exploited intermittently in this area since 1893. Veins range from a few centimetres to a few metres in width, are notably lenticular and contain localized high grade shoots characterized by uneven distribution of gold. The veins are locally sulphide-rich and sphalerite, galena and chalcopyrite commonly are major components. Tourmaline, arsenopyrite and scheelite are rare accessories. Gold-bearing quartz veins are restricted spatially to the southeast domains which have been metamorphosed at low grade (Poulsen 1981) and are found in two structural associations. Most occur within ductile shear zones in plutonic and massive metavolcanics while some occur in dilatant zones parallel with regionally developed cleavage.

Index of Properties

● Properties with moderate production
(<10,000 oz. Au)
1. Golden Star mine

■ Properties with limited production
(<10,000 oz. Au) and/or extensive development
2. Foley mine
3. Olive mine

▲ Properties with limited production
(~1,000 oz. Au) and/or moderate development
4. Pacitto mine
5. Isabella mine
6. Ferguson mine
7. Golden Crescent mine
8. R.C. Cone mine
9. Cone prospect
10. Stagge prospect
11. Alice "A" mine
12. Turtle Tank prospect
13. Saundry mine
14. Young –Corrigan prospect
15. Stellar mine
16. South Vermilion mine
17. McKenzie Gray prospect
18. Dinosaur –Smylie mine
19. Lucky Coon mine
20. Manhattan –Decca mines

△ Properties with limited production
(<100 Au oz. Au) and/or limited development
21. Emma Abbot occurrence
22. Gold Bug occurrence
23. E. Turtle River occurrence
24. W. Turtle occurrence
25. Turtle Siding occurrence
26. McMillan occurrence
27. Corrigan occurrence
28. Thomson occurrence
29. Barber Lake Au occurrence
30. Scott Island occurrence
31. Swell Bay occurrence
32. Emperor mine
33. Gibson occurrence
34. Finger Bay occurrences
35. Stone occurrence

Figure 1. *Geological sketch map of gold properties and major fault structures in the Mine Centre – Fort Frances area. The bars plotted through the symbols reflect the orientation of vein systems on each property.*
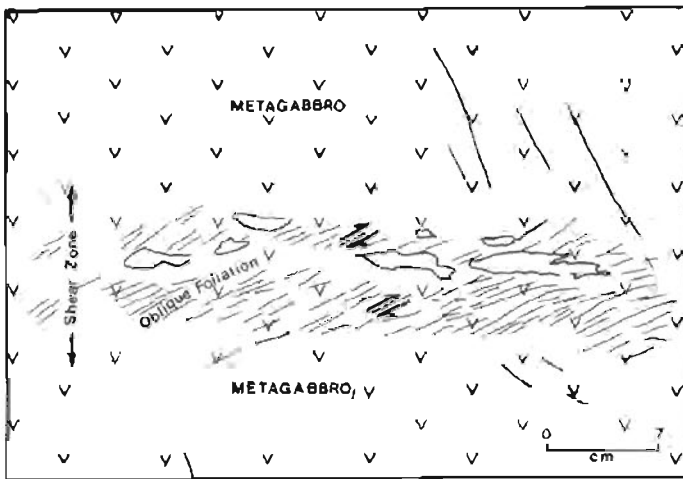
Figure 2. Ductile shear zone cutting metagabbro, Seine Bay. The asymmetry of foliation oblique to the shear zone indicates a dextral sense of shear.
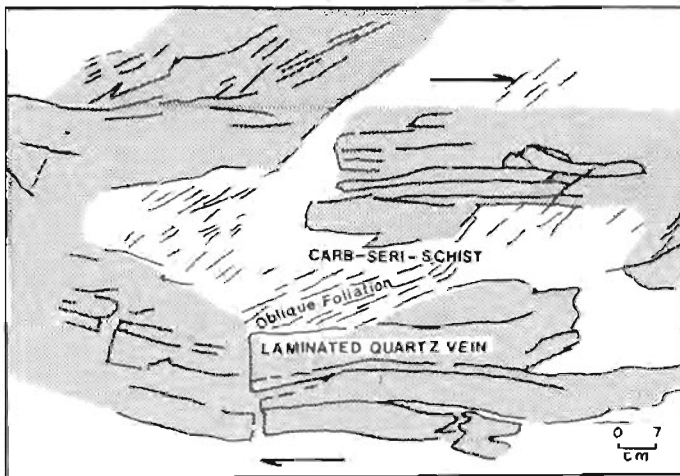

Figure 3. Laminated quartz carbonate in dextral shear zone, Stellar Mine. Note the oblique foliation in carbonate-rich sericite schist derived from the trondhjemite host.
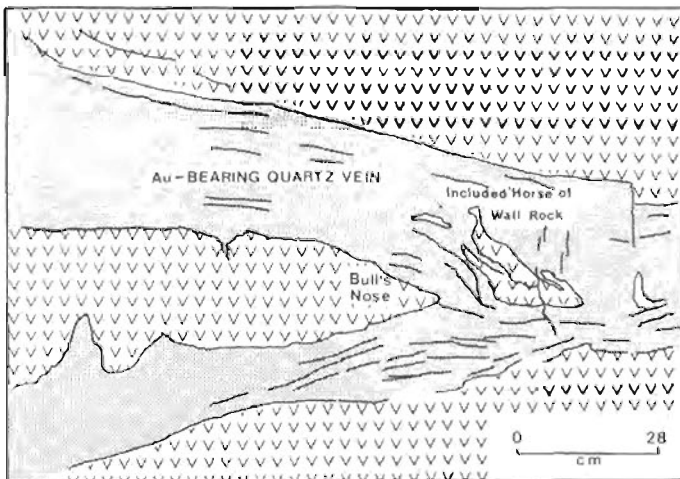

Figure 4. Branching in a shear zone to create a "bull's nose" structure, Manhattan Mine. A narrow zone of foliated rock adjacent to the veins indicates the same dextral shear sense for both branches.
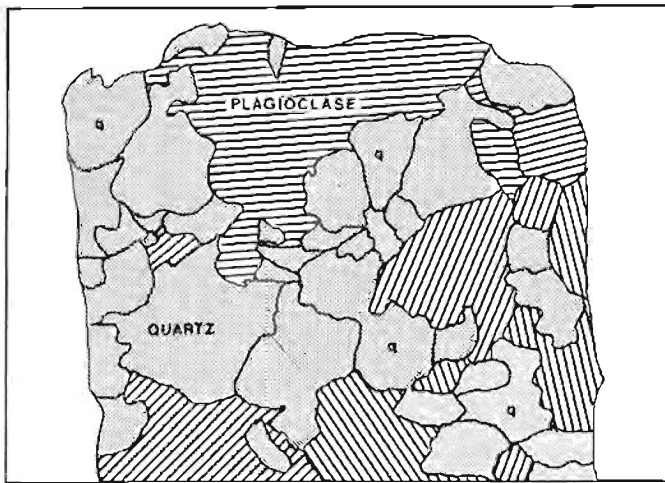
Figure 5. Sketch of thin section of weakly deformed tonalite, Foley Mine area. Note relatively equant and unaltered plagioclase and quartz grains. Width of view approximately 2 cm.

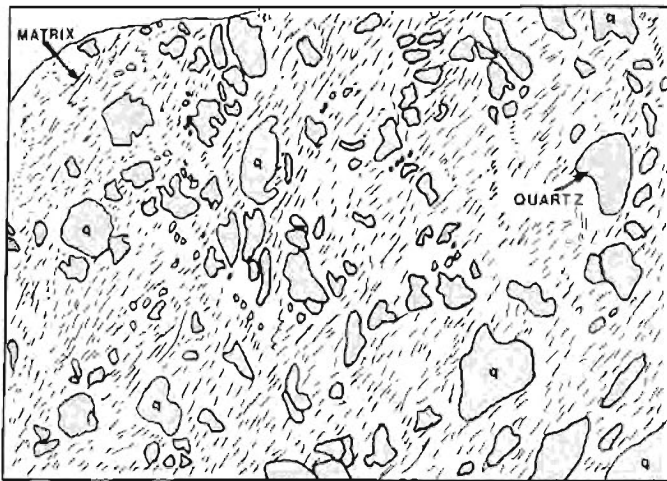**Figure 6.** Sketch of thin section of protomylonite from shear zone in tonalite, Foley Mine area. Note the complete absence of plagioclase with fine grain foliated sericitic matrix in its place. Grain size reduction in quartz is due both to cataclastic and recrystallization processes. Field of view as in Figure 5.
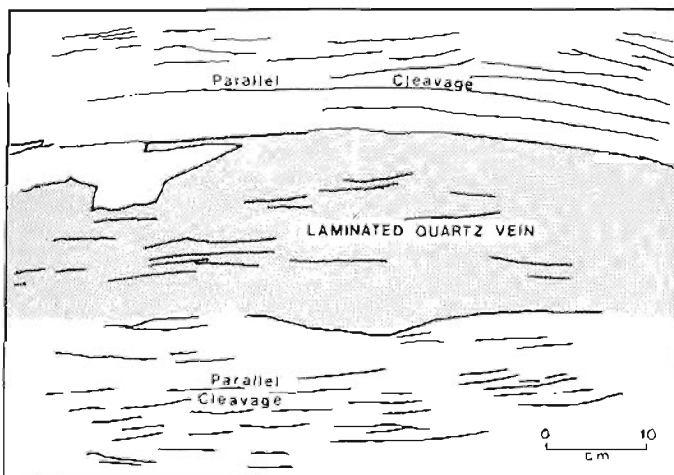

Figure 7. Lenticular, laminated quartz vein parallel to cleavage, Olive Mine.

Ductile shear zones (Ramsay and Graham 1970; Ramsay 1980) are common throughout the Rainy Lake area. They are tabular zones, centimetres to metres wide, which contain an oblique internal foliation in contrast to the homogeneous, equigranular rocks which they transect (Figure 2). Asymmetry of foliation, sigmoidal second order vein arrays, discrete slip surfaces with slickensides and rare offset of markers provide evidence for subhorizontal displacements parallel to the shear zone boundaries. The gold-bearing quartz veins most commonly occur in the central part of a shear zone (Figure 3). Branching of shear zones produces the common "bull's nose" structure (Figure 4) and included "horses" of wall rock within veins. The foliated wall rocks which comprise the shear zones show abundant evidence of mechanical and chemical alteration. For example, equigranular tonalites and trondhjemites away from a shear zone (Figure 5) give way gradationally to schists and protomylonites in which feldspars have been converted entirely to foliated sericitic matrix, and quartz porphyroclasts show abundant evidence of grain size reduction (Figure 6). The width of foliated rock developed on either side of a vein varies from centimetres to metres; there is no direct relationship between vein width and shear zone width, yet the widest shear zones appear to be most persistent along strike. Misoriented inclusions of foliated wallrock occur locally within veins and the laminated nature of the veins themselves (see Figure 3) results from narrow sericitic or chloritic inclusions of wallrock incorporated into them. These textures are interpreted to be the result of episodic brittle failure at the interface between early vein material and foliated wallrock followed by new vein filling at that site. Portions of veins which are finely laminated generally are richer in gold than those which are the coarse grained products of a single vein filling episode.

The shear zones are demonstrably related in a kinematic sense to regional wrench faulting. Their vertical orientation, vertical foliation, subhorizontal slickensides and the geometry of sigmoidal vein arrays indicate dominantly transcurrent displacements. Dextral shear zones are most abundant adjacent to the late, bounding dextral faults, and conjugate sinistral structures are found most commonly in the central part of the area (see Figure 1). Westerly striking shear zones are all dextral while northwesterly to northerly striking zones are sinistral, compatible with the overall dextral nature of the regional wrench zone (Poulsen 1981; Blackburn et al. 1982). The shear zones cut all rock types but are found most commonly in tonalite and trondhjemite (Poulsen 1981), an observation which led early workers to relate gold mineralization to emplacement of intrusions of this composition. An important observation, however, is that metamorphosed basalt, diabase and gabbro also host shear zones and veins and that the orientation and shear sense of the zones is independent of the orientation and facing directions of the rock units which they cut; they are, therefore, late, superimposed discordant structures.

A second structural association for gold is exemplified by the Olive Mine and several smaller prospects and occurrences of similar type (see Figure 1). The host rocks, in this case, are tuffs and metasediments with well developed cleavage. Laminated veins parallel this cleavage (Figure 7) and likely result from decoupling of cleavage laminae by shear displacement. Locally, folding and brecciation of the host rock gives rise to irregular vein networks associated with longer, sigmoidal cleavage-parallel veins. While morphologically different from the shear zones, formation of these types of vein is thought to be merely the response of anisotropic host rocks to shear displacement in a tectonic wrench zone.

WABIGOON SUBPROVINCE
GOLD DISTRIBUTION AND FAULT ZONES

Figure 8 shows the distribution of gold deposits of the Wabigoon Subprovince relative to the positions of regional faults. It is evident that the fault network described in the Mine Centre – Fort Frances area extends eastward along the subprovince margin through the Atikokan, Beardmore and Geraldton areas. The bulk of gold production from the subprovince has come from the latter district where the locus of mineralization is the east-striking Bankfield-Tombill Fault (Horwood 1948). A second fault network which lies internal to the subprovince comprises the Miniss-Wabigoon-Manitou Lakes Fault Zone along which there is also a very prominent association of vein-type gold deposits. The fault and shear zone networks of the Wabigoon Subprovince consist of two distinct elements: east-trending dextral faults and conjugate faults striking 030° reflect a late-tectonic shortening of the subprovince about a northwesterly trending axis (Schwerdtner et al. 1979; Park 1981). Shorter faults of differing orientation are likely second-order splays (McKinstry 1953) of the principal fault zones. The localization of gold in subsidiary structures related to the fault zones in the Wabigoon Subprovince implies an equally late timing for their formation.

RECOGNITION OF THE FAULT ZONES

The fault zones identified on Figure 8 come from compilation maps of the Ontario Geological Survey. The most significant of the structures mark dramatic stratigraphic discordances and generally have been recognized as fault zones from the time of earliest mapping. Potential exists, however, for the recognition of new or related structures of lesser dimension. Identification of fault rocks (Sibson 1977) provides a useful criterion for recognition of faults: mylonite, cataclasite, phyllonite and pseudotachylite have distinctive petrographic characteristics. Minor structures such as asymmetric folds and minor sympathetic brittle faults are commonly localized in the vicinity of major faults. Anastamosing fault networks isolate characteristic lozenge-shaped domains (see Figure 1). Electromagnetic anomalies and topographic lineaments also commonly mark fault zones. The above criteria certainly apply in the Mine Centre – Fort Frances area and at other localities in the Wabigoon Subprovince (Blackburn et al. 1982; Poulsen and Franklin 1981).
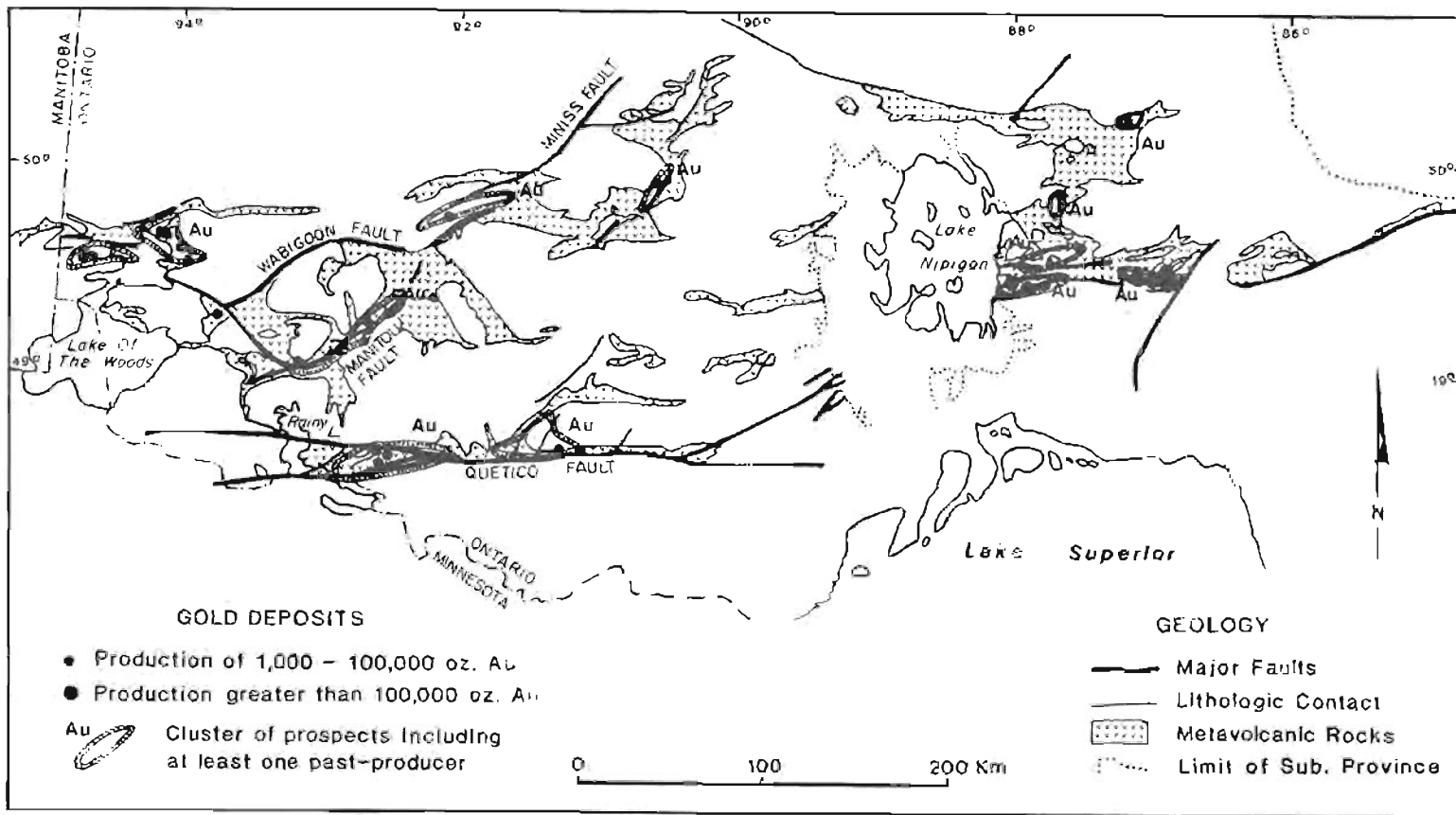
Figure 8. *Distribution of gold deposits and fault zones in Wabigoon Subprovince. Deposits with past production in excess of 1000 ounces of Au are shown*

GOLD DEPOSITS

- Production of 1,000 – 100,000 oz. Au
- Production greater than 100,000 oz. Au

Au ⬭ Cluster of prospects including
    at least one past-producer

GEOLOGY

— Major Faults
— Lithologic Contact
▦ Metavolcanic Rocks
⋯ Limit of Sub. Province

0   100   200 Km

IMPLICATIONS FOR EXPLORATION AND GENETIC MODELS

The above observations imply that much of the gold exploited to date in the Wabigoon Subprovince has come from fault-related structures, both on the regional and local scales. While it is not suggested that structural siting is the only requirement for lode gold mineralization, it is proposed that recognition of potential fault structures should represent one criterion in target selection for gold in the Wabigoon Subprovince. The genetic significance of the observed relationship remains speculative. The relationship may be indirect in that the faults and other commonly related features such as shallow-water conglomerate and felsic intrusions merely reflect a common tectonic environment in which gold is localized in passive conduits by other magmatic or metamorphic processes. A more likely relationship is that regional faults are directly responsible for the transport of fluids in their vicinity. Sibson *et al.* (1975) have used theoretical considerations to show that "seismic pumping" is a viable explanation for the direct observation of warm fluids which are commonly expelled from active fault zones. Fluids may be of magmatic, meteoric or metamorphic origin but major fault zones have the potential for involving large fluid volumes including those from deep crustal sources. The apparent control of metamorphic grade on the localization of gold in the Mine Centre – Fort Frances area suggests that fluids derived from metamorphic dehydration (Fyfe and Henley 1973) may be significant in this example. The application of the above model to lode gold deposits of the Mine Centre – Fort Frances area and possibly of the Wabigoon Subprovince as a whole implies that they are relatively late stage epigenetic features.

REFERENCES

Blackburn, C.E., Breaks, F.W., Edwards, G.R., Poulsen, K.H., Trowell, N.F., and Wood, J.
1982: Stratigraphy and Structure of the Western Wabigoon Subprovince and Its Margins, Northwestern Ontario; Geological Association of Canada, Field Trip Guide Book, Winnipeg, 105p.

Borradaile, G.J.
1982: Comparison of Archean Structural Styles in Two Belts of the Canadian Superior Province; Precambrian Research, Vol. 19, p.179-189.

Fyfe, W.S., and Henley, R.W.
1973: Some Thoughts on Chemical Transport Processes, with Particular Reference to Gold; Minerals Science and Engineering, Vol. 5, p.295-302.

Horwood, H.C.
1948: General Structural Relationships of Ore Deposits in the Little Long Lac-Sturgeon River Area; p.377-384 in Structural Geology of Canadian Ore Deposits, Vol. 1, Canadian Institute of Mining and Metallurgy.

McKinstry, H.E.
1953: Shears of the Second Order; American Journal of Science, Vol. 251, p.401-404.

Park, R.G.
1981: Shear Zone Deformation and Bulk Strain in Granite-Greenstone Terrain of the Western, Superior Province, Canada; Precambrian Research, Vol. 14, p.31-48.

Poulsen, K.H.
1981: The Geological Setting of Mineralization in the Mine Centre – Fort Frances Area, District of Rainy River; p.190-195 in Summary of Field Work, 1981, by the Ontario Geological Survey, edited by J. Wood, O.L. White, R.B. Barlow, and A.C. Colvine, Ontario Geological Survey, Miscellaneous Paper 100, 255p.

Poulsen, K.H., Borradaile, G.J., and Kehlenbeck, M.M.
1980: An Inverted Archean Succession at Rainy Lake, Ontario; Canadian Journal of Earth Sciences, Vol. 17, p.1358-1369.

Poulsen, K.H., and Franklin, J.M.
1981: Copper and Gold Mineralization in an Archean Trondhjemitic Intrusion, Sturgeon Lake, Ontario; p.9-14 in Current Research, Part A, Geological Survey of Canada, Paper 81-1A.

Ramsay, J.G.
1980: Shear Zone Geometry: a Review; Journal of Structural Geology, Vol. 2, p.83-99.

Ramsay, J.G., and Graham, R.H.
1970: Strain Variation in Shear Belts; Canadian Journal of Earth Sciences, Vol. 7, p.786-813.

Schwerdtner, W.M., Stone, D., Osadetz, K., Morgan, J., and Stott, G.M.
1979: Granitoid Complexes and the Archean Tectonic Record in the Southern Part of Northwestern Ontario; Canadian Journal of Earth Sciences, Vol. 16, p.1965-1977.

Sibson, R.H.
1977: Fault Rocks and Fault Mechanisms; Journal of the Geological Society of London, Vol.133, p.191-213.

Sibson, R.H., Moore, J.M., and Rankin, A.H.
1975: Seismic Pumping — a Hydrothermal Fluid Transport Mechanism; Journal of the Geological Society of London, Vol.131, p.191-213.

Wood, J.
1980: Epiclastic Sedimentation and Stratigraphy in the North Spirit Lake and Rainy Lake Areas: A Comparison; Precambrian Research, Vol.12, p.227-255.

# APPENDIX B CDS PROCESSING

What is a CDI?

The term CDI is short for **C**onductivity **D**epth **I**maging. The purpose of CDI processing is to convert multichannel EM data[1] into the equivalent conductivity distribution in the earth that would produce the observed EM response. While the program assumes the earth is layered (meaning all changes in conductivity are vertical), by processing many points along a line and then gridding the result, a two dimensional (or three dimensional if gridded again) approximation of the earth's conductivity can be obtained. The results of CDI processing are then displayed in a CDS, short for **C**onductivity **D**epth **S**ection (central image in the figure below).
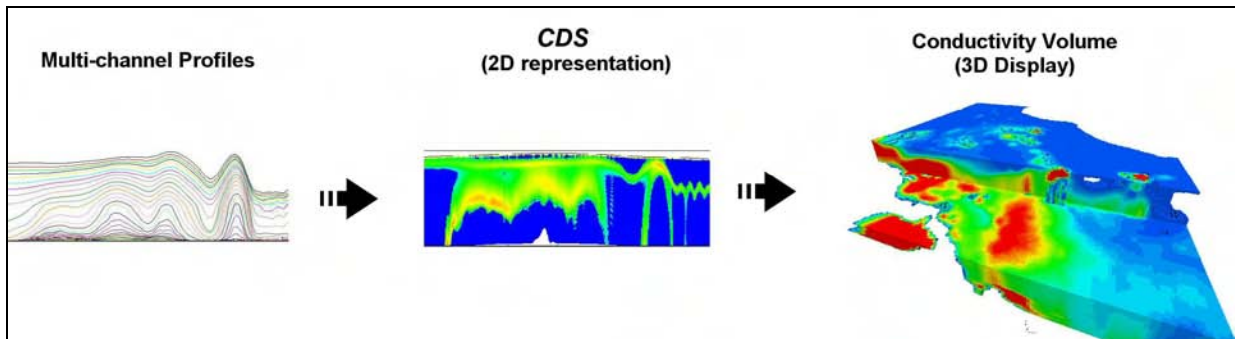
In what would be termed a simple conductivity environment where all conductors are expected to be steeply dipping in a resistive host rock, CDI processing will not likely add much new information when making target assessments. However, in many situations the target conductivity may be caused by a mixture of massive and disseminated sulfides and CDI processing will enhance the likelihood of being able to map the overall conductivity distribution much like IP surveying has been used historically in VMS exploration. Also, if the overburden is conductive and/or has a variable thickness, CDI processing helps to identify such changes and reduces the potential ambiguity of mistaking variations in the overburden for targets of interest in the bedrock.


---
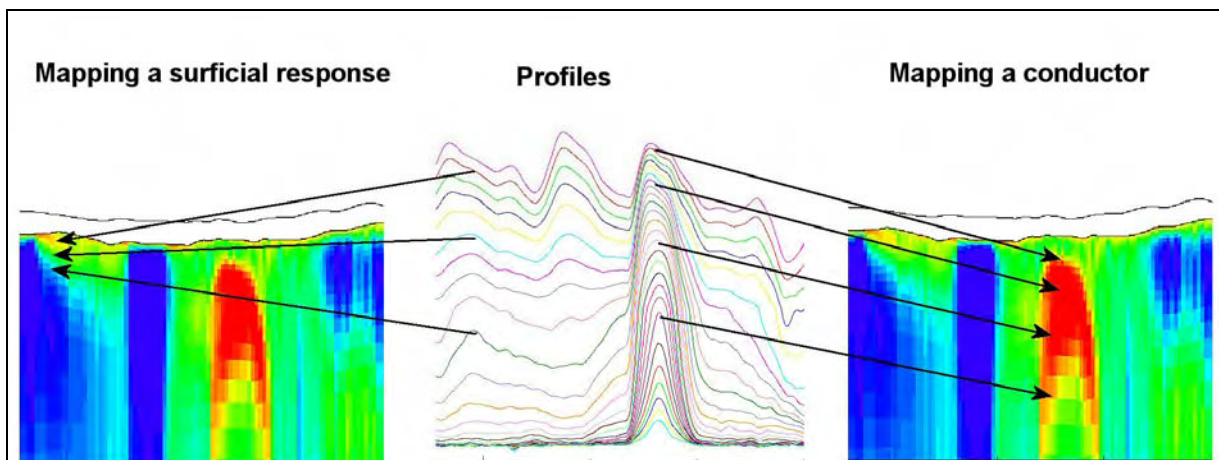
[1] Time domain CDIs are discussed here but the same process can as well be applied to frequency domain data as well, this is discussed under a companion Technical Note

Condor Consulting, Inc.   September 2005   Condor Technical Note-CDI TD

# APPENDIX C BACKGROUND ON ADTAU

Time Constant Analysis
AdTau

The AdTau program calculates the time constant (tau) from time domain decay data. The program is termed **AdT**au since rather than using a fixed suite of channels as commonly done, the user sets a noise level and depending on the local characteristics of the data, the program will then select the set of last five channels that are above this noise level. In resistive areas, the earlier channels will tend to be used (i.e. little late time response), whereas in conductive terrains the latest channels available can generally be used. A typical decay fit is shown on the right.
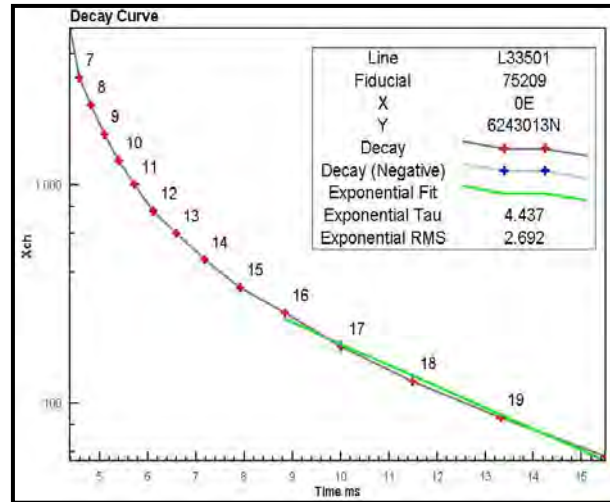
Below is an image showing the benefit of examining time constant over simple EM amplitudes. On the top is an image of early time EM data. Two zones are highlighted. Feature A is a large area of response with a few modest isolated highs that are bracketed by two strong linear trends. The AdTau image shows this zone to be strongly conductive and made
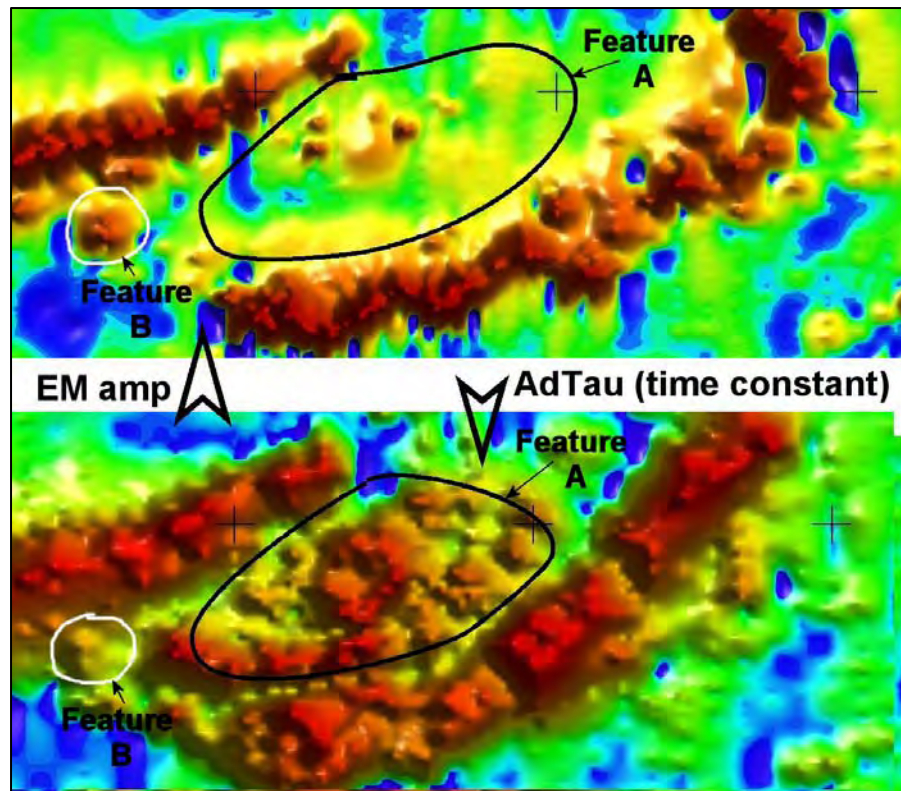
up of a number of discrete sources. Feature B on the other hand appears in the EM amplitude plot to be a strong discrete feature. In the AdTau display however, it is apparent that this feature is not particularly conductive compared to other sources in the area. As well, the AdTau image shows that western part of the feature is more conductive.

APPENDIX D ZS FILTERING

New enhancement filters for geological mapping

Zhiqun Shi*
Encom Technology Australia
zhiqun.shi@encom.com.au

Graham Butt
Encom Technology Australia
graham.butt@encom.com.au

SUMMARY

Two types of filters have been developed for the purpose of enhancing weak magnetic anomalies from near-surface sources while simultaneously enhancing low-amplitude, long-wavelength magnetic anomalies from deep-seated or regional sources. The Edge filter group highlights edges surrounding both shallow and deeper magnetic sources. The results are used to infer the location of the boundaries of magnetised lithologies. The Block filter group has the effect of transforming the data into "zones" which, similar to image classification systems, segregate anomalous zones into apparent lithological categories. Both filter groups change the textural character of a dataset and thereby facilitate interpretation of geological structures.

The effect of each filter is demonstrated using theoretical model studies. The models include both shallow and deep sources with a range of magnetisations. Comparative studies are made with traditional filters using the same theoretical models. In order to simulate real conditions, Gaussian noise has been added to the model response. Techniques for noise reduction and geological signature enhancement are discussed in the paper.

The new approaches are applied to actual magnetic survey data covering part of the Goulburn 1:100 000 scale map sheet area, New South Wales. Some new geological inferences revealed by this process are discussed

Key words: Enhancement filters, magnetic sources, geological mapping.

INTRODUCTION

High-resolution aeromagnetic survey data represent a rich source of detailed information for mapping surface geology as well as for mapping deep tectonic structure. Traditional enhancement techniques, such as first vertical and horizontal derivatives (1VD, 1HD), analytic signal (AS), and high-pass in-line or grid filters are used in enhancing magnetic anomalies from near-surface geology.

In recent years the potential field tilt filter has been introduced (Miller and Singh, 1994) and it has achieved recognition for its value in the analysis of potential field data for structural mapping and enhancement of both weak and strong magnetic anomalies (Verduzco *et al*, 2004). The total horizontal derivative of the TMI reduced to the pole is also widely used for detecting edges or boundaries of magnetic sources (Cordell and Grauch, 1985; Blakely and Simpson, 1986; Phillips, 1998).

Several disadvantages pertain to the use of these traditional filters. They often only diffusely identify source location and boundaries, particularly in colour image presentations. They usually emphasise short wavelength anomalies at the expense of signal from deeper magnetic sources and the range of amplitudes remaining in the filtered output may dominate the source boundary information being sought. In addition, some traditional filters emphasise noise with resultant impact on the interpretation of source boundaries.

This paper identifies new processes which have been developed to address these disadvantages and provide output which can improve map-based interpretations.

Unless otherwise stated, all filters have been operated on TMI data reduced to the pole (RTP).

METHOD AND RESULTS

Theoretical Model Testing

A theoretical 2D grid of total magnetic intensity (TMI) computed at the surface was created by forward 3D modelling of the TMI response from a set of theoretical magnetic sources having variable width, strike extent, depth, depth extent (DE), dip, magnetic susceptibility and strike azimuth. A list of these parameters is presented in Table 1. In two of the sources, remanence was simulated using negative magnetic susceptibility. The TMI of the theoretical models was computed at a geomagnetic inclination of -60 degrees using a notional east–west line spacing of 200 m and a grid cell size of 40 m. The TMI grid was then reduced to the pole (RTP) (Figure 1).
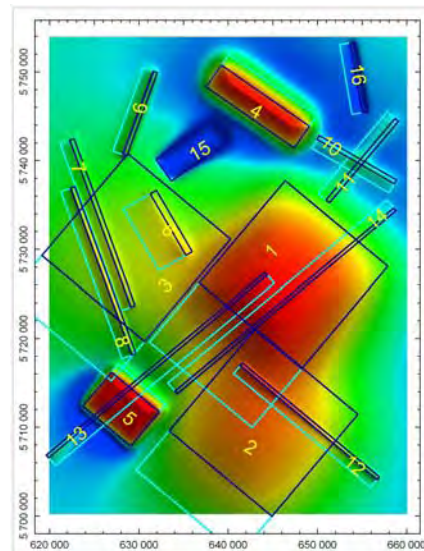

Figure 1. RTP image derived from multiple theoretical 3D magnetic sources, shown as wire frame outlines

A set of traditional filters was operated on the theoretical RTP grid. They include AS, 1VD, modulus of horizontal derivatives (MS) and Tilt and the results are presented in

Figure 2. The output grids variously show discontinuous trending (crossed sources in upper right of AS image), diffuse, weak edges (deep source in centre right of the MS image) and lack of precise source edge definition (1VD and Tilt).

Model Label	Depth (m)	Width (m)	DE (m)	Dip (deg)	Magnetic Susceptibility (SI)	Strike Length (m)	Azimuth (deg)
1	4000	15000	15000	120	0.010	15000	-050
2	6000	15000	10000	120	0.010	15000	-050
3	10000	15000	10000	120	0.010	15000	-050
4	1000	3000	4000	70	0.010	12000	-055
5	500	5000	2000	60	0.010	7000	-050
6	1000	800	2000	150	0.005	8000	-030
7	600	500	2000	120	0.001	20000	-020
8	200	500	2000	120	0.001	20000	-020
9	500	500	2000	120	0.003	10000	020
10	1000	500	2000	120	0.003	20000	-060
11	1000	500	2000	120	0.003	12000	040
12	200	400	2000	120	0.001	20000	-050
13	500	400	1000	40	0.002	32000	050
14	500	400	1000	140	0.001	32000	050
15	600	3000	4000	90	-0.002	8000	055
16	400	600	2000	120	-0.010	8000	-010

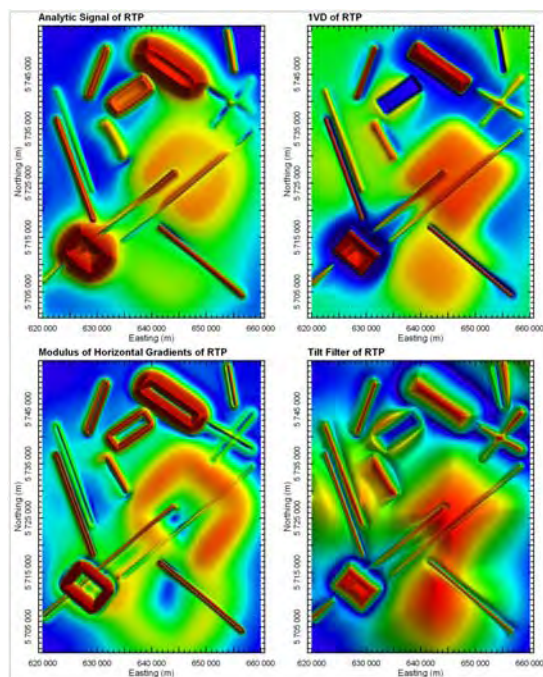**Table 1. List of parameters of theoretical magnetic sources**

Figure 2. Comparison of enhancement filters of RTP: AS, 1VD, MS and Tilt filter. The models used are those depicted in Figure 1.

Edge Filters

The first avenue of development was to increase the sharpness of the anomalies used to map the edge of the magnetic sources. The MS grid yields anomaly peaks over the source edge locations, whereas these edges coincide with gradients in the 1VD, Tilt and AS filtered outputs. None of these filters produces easily interpreted edges in image form when the sources are weakly magnetised or are deep.

A new linear, derivative-based filter termed the ZS-Edgezone filter has been developed to improve edge detection in these situations. Its effect is shown in Figure 3 using the same theoretical models discussed earlier. The advantages of the filter are greatly increased anomaly sharpness over source edges and compression of the amplitude range so that differences in the original TMI amplitudes do not persist to

dominate the edge interpretation. This has the ancillary effect that the method can be modified to provide automated edge conversion to vectors for use in GIS systems.

Although this filter significantly improves the precision of edge determination, it is subject to normal potential field limitations which determine that source edges cannot be resolved where the source is narrow relative to its depth. The filter also can produce a "halo" type artefact due to superposition of the response of a limited depth extent shallow source (Figure 1, Model 6) on that of deeper sources. A similar "halo" effect can be seen around the edges of remanently magnetised Model 15, also in Figure 1.

The ZS-Edge filter (Figure 4) has also been developed to map source edges. This filter differs from the ZS-Edgezone filter in that a greater contribution of the TMI anomaly amplitude over the source is retained, thereby improving anomaly characterisation at the expense of edge sharpness.

Both these filters produce edges which migrate down-dip towards the deepest edge of the source. This effect produces anomaly asymmetry that can assist interpretation of dip, although this effect is more pronounced for the ZS-Edge filter than for the ZS-Edgezone filter. Down-dip source extensions are depicted in cyan in Figure 1.
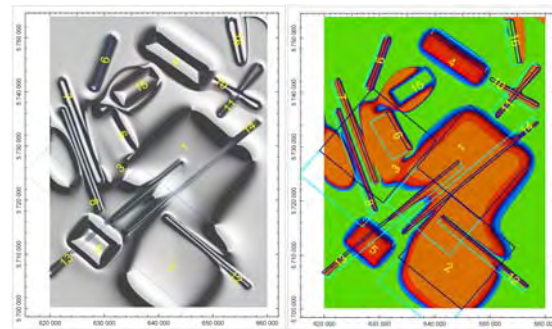

Figure 3. Anomaly edge and block enhancements using the ZS-Edgezone (left) and ZS-Block filters (right). Model positions are shown using wire frames.

Block Filters

In attempting to improve edge detection filters, an obvious progression is to highlight the magnetic regions whose edges have been mapped. To do this, a set of filters called "block" filters has been developed.

The Block filter group has the effect of transforming the potential field data into "zones" which, similar to image classification systems, segregate anomalous zones into apparent lithological categories. These filters can be imported for use in image classification systems or displayed in RGB space with other grids for empirical classification purposes.

The block filters, like the edge filters, are linear, derivative-based filters which use a combination of derivative and amplitude compression techniques to render the magnetic data into regions whose edges are sharply defined and whose amplitudes have a reduced range in comparison to the original TMI.

The ZS-Block filter (Figure 3) and the ZS-Plateau filter (Figure 4) depict the magnetic data as a 2D plan of apparent magnetic source distribution. Artefacts may occur as discussed for the edge filters.

The choice of ZS-Block, ZS-Plateau or ZS-Area filters will depend on the data characteristics of each magnetic survey and on the end-use requirement. The ZS-Plateau filter, for example, yields less variation in amplitude "texture" over a magnetic unit that either the ZS-Block or ZS-Area filters.
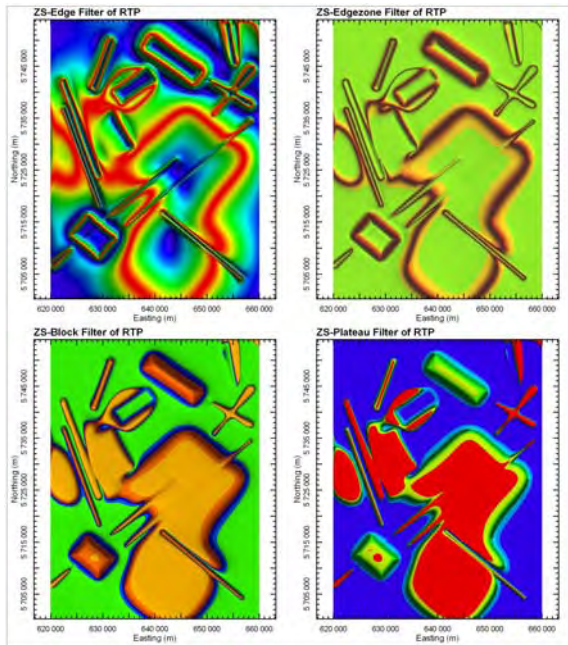

Figure 4. Comparison of ZS-Edge, ZS-Edgezone, ZS-Block and ZS-Plateau filtered outputs of RTP data

Effects of Noise

The influence of noise on the operation of these enhanced grids was tested by adding a large component of noise to the theoretical TMI profile data. This noise had a Gaussian distribution with a standard deviation equal to ten percent of the TMI standard deviation. The noise-modified TMI profile data were then de-spiked using a non-linear technique. Both the noise-affected and the de-spiked TMI data were then gridded and converted to RTP. The RTP data were then processed both with the traditional and newly developed filters.

Figure 5 shows the effect of the noise on the computations. The image of the noise-affected 1VD RTP data (top right) shows that weak and deep sources have been severely masked by the noise. Significant improvement can be achieved by using de-spiked data (lower left) or by low-pass grid filtering — for example, using an upward continuation filter (lower right).

Figure 6 shows that if real data with significant noise is encountered, a standard de-spiking or low-pass smoothing procedure may be used to achieve successful application of both the traditional and newly developed filters.

Figure 6 also depicts the use of enhanced outputs in RGB space to provide examples of how the combination of amplitude information (red colour) with edge information (green and blue colours) can be used to highlight source boundaries and remanence in a single image.
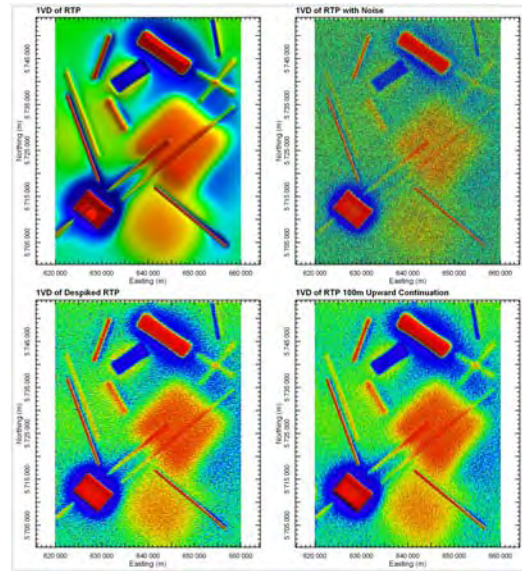

Figure 5. Comparison of 1VD of original model RTP data (top left) with noise-affected RTP data (top right) and noise-reduced RTP data (lower images)
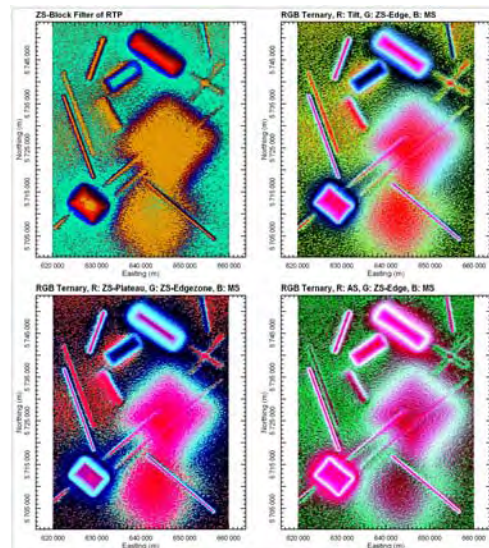

Figure 6. ZS-Block filter using noise-reduced RTP data (top left) and examples of filter combinations in RGB space using noise-reduced RTP data

Application to Field Data, Goulburn 1:100 000 Scale Map Sheet Area, New South Wales

Both the traditional and new enhancement filters were applied to test their suitability for geological definition to airborne magnetic survey data over the Goulburn 1:100 000 scale map sheet area (Johnson *et al,* 2003). These data were acquired as part of a joint program between the NSW Department of Mineral Resources and Geoscience Australia, with 250 m–spaced east–west flightlines. The magnetometer sensor occupied a nominal terrain clearance of 80 m. This dataset was selected since new detailed geological mapping had been recently completed. All the enhancements have been computed using TMI data reduced to the pole.

Figure 7 shows a comparison of part of the Goulburn 1:100 000 map sheet area surface geology with the ZS-Area

filter output. In the area surrounding location C, the ZS-Area filter transforms the magnetic data into separate magnetic units, which comprise the Devonian Bindook Volcanic Complex. The magnetic regions correlate closely with mapped andesites (Dkqa–cream coloured unit in Figure 7) whilst the intervening less-magnetic units correlate with rhyolitic ignimbrites (Dkqy–red unit in Figure 7)
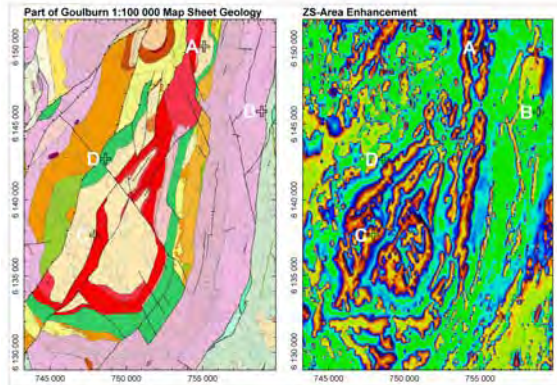

Figure 7. Comparison of geology and ZS-Area enhancement over the Bindook Volcanic Complex

Figure 8 displays some of the advantages of the edge detection filters. At location A, ambiguity concerning the continuity of Quialigo Formation units (cream and red units in Figure 7) is resolved by the ZS-Edgezone filter. At location B, a subtle lineament is confirmed, whilst at location D, the extent of the Bullamalita Conglomerate (green unit in Figure 7) is clearly mapped by the ZS-Edge filter. Structural breaks are often more easily interpreted using these transforms, for example, immediately southwest of location D.
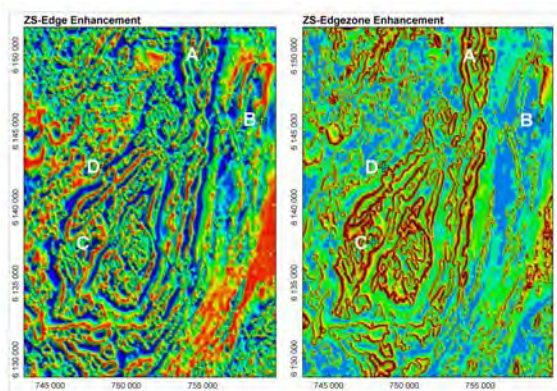
Figure 8. Comparison of ZS-Edge and ZS-Edgezone enhancements over the Bindook Volcanic Complex

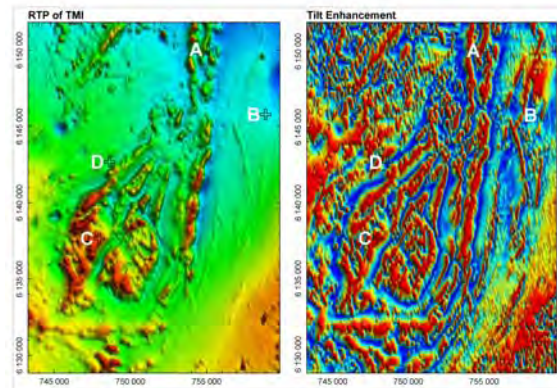Figure 9 shows standard RTP and Tilt transforms over the same area for reference.

Figure 9. Comparison of RTP and Tilt filters over the Bindook Volcanic Complex

CONCLUSIONS

Traditional filters used to enhance magnetic data, including the more recently developed potential field tilt filter, are currently used to assist in determination of the location and extent of magnetic units.

Newly developed derivative-based filters may be used to improve the precision of source edge detection and, by extension, the determination of the spatial extent of magnetic units. These filters are demonstrated to perform successfully on both strongly magnetised features as well as on weakly magnetised or deep magnetic features. Artefacts may result particularly where anomaly superposition occurs.

The impact of noise in real data may be accommodated by these new methods provided noise-reduction techniques are employed.

The new filter outputs may be used as part of regional or detailed geological mapping projects, including in classification systems or in RGB space, to improve lithological discrimination and mapping.

The speed of magnetic unit mapping can be considerably increased through reliance on edge detection filters. Further improvements in mapping speed can be envisaged through automated conversion of edge anomalies to vector files.

ACKNOWLEDGMENTS

REFERENCES

Blakely, R. J. and Simpson, R. W., 1986, Locating edges of source bodies from magnetic or gravity anomalies, Geophysics, 51, 1494-1498.

Buckingham, A.J, Dentith, M.C., and List, R.D, 2003, Towards a system for content-based magnetic image retrieval: Exploration Geophysics, 34, 195-206.

Cordell, Lindrith, and Grauch, V.J.S., 1985, Mapping basement magnetization zones from aeromagnetic data in the San Juan Basin, New Mexico pp.181-197. In Hinze, W.J., ed,. The utility of regional gravity and magnetic maps: Society of Exploration Geophysicists,

Johnson A.J. *et al.*, 2003, Goulburn 1:100 000 Sheet 8828 Geology Map, New South Wales Department of Mineral Resources.

Miller, H.G., and Singh V., 1994, Potential field tilt — a new concept for location of potential field sources: Journal of Applied Geophysics, 32, 213-217.

Phillips, J.D., 1998, Processing and interpretation of aeromagnetic data for the Santa Cruz Basin–Patagonia Mountains Area, South-Central Arizona: United States Geological Survey Open-File Report 02-98.

Verduzco, B., Fairhead, J. D., Green, C. M., and MacKenzie, C., 2004, New insights into magnetic derivatives for structural mapping: The Leading Edge, 23 (2), 116-119.

APPENDIX E MAGNETIC MODELING DOCUMENTATION AND RESULTS

encom◆ modelvision

Mineral Exploration

The magnetic and gravity methods are used widely in exploration for base metals, gold and other precious metals, diamonds and mineral sands.

Base Metal Exploration
ModelVision is used by mineral exploration companies in most parts of the world because it has the ability to model complex geological shapes in three dimensions with a minimum of effort. The combined use of gravity and magnetic methods makes it possible to deduce many geological factors about a potential deposit prior to drilling.

Diamond Exploration
ModelVision is used by diamond explorers to model magnetic targets believed to be associated with kimberlite pipes.

Gravity data is often used with the magnetic method and simultaneous modelling of gravity and magnetic data helps geologists design optimised drilling programs.

Hazard Assessment

Intrusions within coal mines cause major disruption to coal production and degrade coal quality. Early detection through the use of magnetic data can save millions of dollars in lost production.

ModelVision is used to assess intrusive dykes, sills, plugs and diatremes. It is also used in the interpretation of landfill, buried drums and UXO investigations.

Groundwater

Gravity is used to map the location of buried channels and the magnetic method can detect the depth of cover where the channels are sitting on a magnetic basement. Use both gravity and magnetic modelling with inversion to build a 3D model of buried river channels, deep leads and groundwater basins.

Note: The 3D examples below illustrate ModelVision interpretations in Encom Profile Analyst.

Petroleum Exploration

ModelVision is used to analyse depth to crystalline basement of salt diapirs, seismic controlled layered sequences and micromagnetic features caused by magnetic hydrocarbon indicators.

Depth to Crystalline Basement
Gravity and magnetic surveys are used to help understand under-explored petroleum basins. Even in mature basins, magnetic data is being used to re-evaluate basement structural controls that may have influenced the evolution of the sedimentary section.

Seismic Horizon Integration
You can use depth-converted images of seismic data as backdrops in your section to constrain your interpretation or import seismic horizon data as horizon grids or horizon sections.

Full section modelling using the polygroup body makes it easy to perform joint modelling of the magnetic and gravity data.
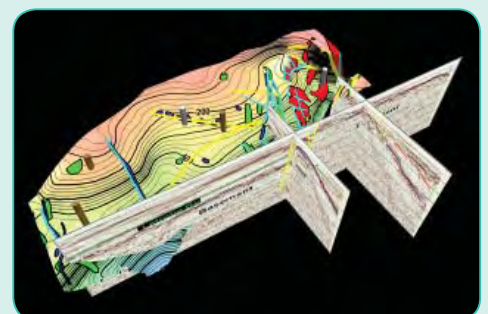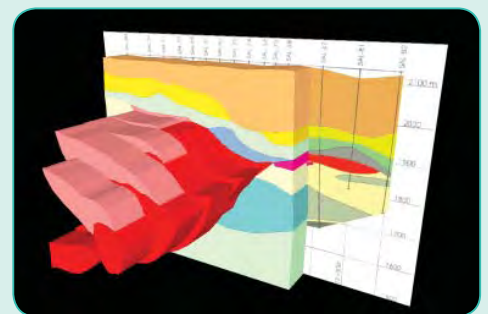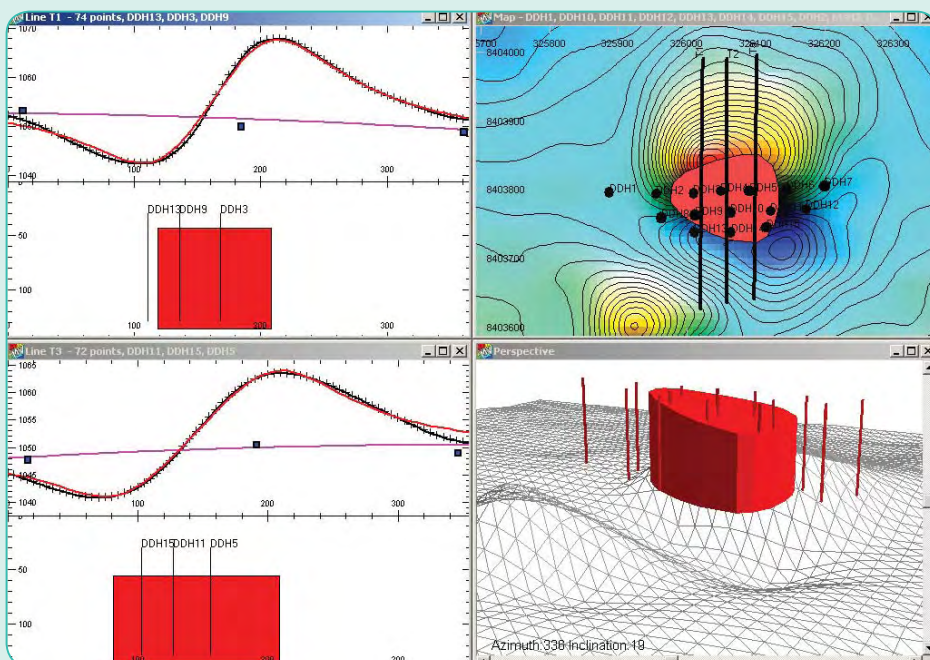
encom⋆ modelvision

Survey Planning & Research

ModelVision models gravity and magnetic data for any 3D model at any x,y,z spatial location including the ground surface, airborne surveys and drillholes. ModelVision is renowned for its ability to interpret 3D potential field data and you can use it to simulate a survey for a wide range of geological models and a wide range of survey types. Instrument types include total field, fluxgate, gradiometers, full tensor magnetometers, gravity, gravity gradiometers and full tensor gravity gradiometers.

ModelVision has a synthetic line and drillhole calculator that creates pre-determined sample locations for modelling. In the case of an airborne survey use a terrain model to derive the local elevation along the line and offset it vertically to create the necessary terrain clearance. You can apply a damping filter to the clearance to simulate the characteristics of the aircraft.

Around the world, geoscience organisations use ModelVision to research issues from processing through to the detectability of subtle buried targets. It is used in research and teaching for introductory training in geophysics through to the solution of advanced research problems. When combined with the synthetic survey capability almost any geoscience interpretation problem can be simulated.

Airborne contractors and QC personnel use ModelVision to analyse daily results and simulate the expected responses from detailed surveys with 50m line spacing to regional surveys with 1km line spacing. ModelVision is packed with features designed to solve the great diversity of geological problems that are suited to magnetic and gravity investigations.

2D/3D Modelling

ModelVision performs all modelling in 3D but provides the operational efficiency of 2D modelling by providing optimised cross-sections.

Guided 3D Inversion

ModelVision user-guided inversion supports your geological modelling by allowing you to select individual parameters for refinement.

ModelVision supports single profile inversion for isolated cross-sections and full 3D inversion of multiple lines of data. With modern GPS surveying you can invert on data collected along multiple lines with computations made at the elevations of the sample locations.

Active Point mode allows you to select a subset region in a map or cross-section. You can model part of a large survey without having to model every property, vertex position, dip, strike, remanence vector etc.
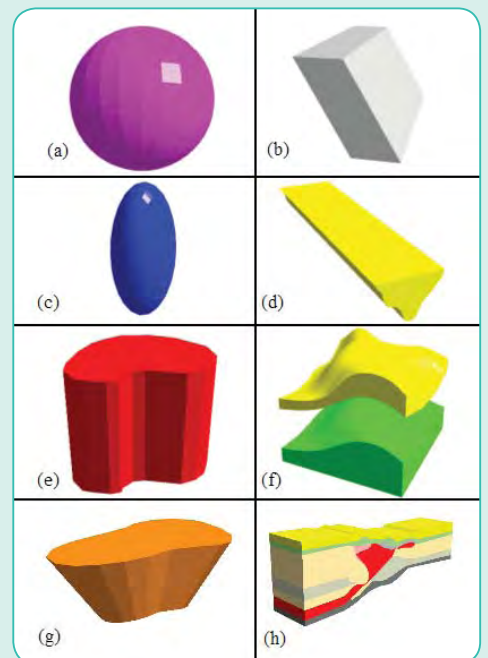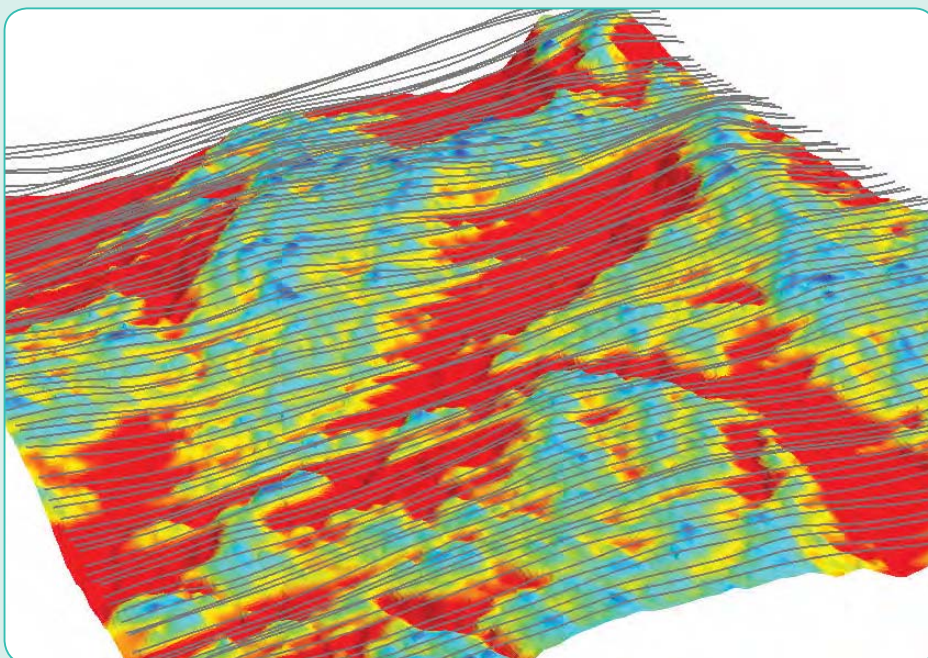
encom◆ modelvision

Gravity & Magnetic Gradiometer Simulation

ModelVision models the full gravity tensor so you can model data collected by the BHP Billiton FalconTM or Bell Geospace airborne gravity gradiometer systems.

You can simulate total field magnetic gradiometer surveys for the next generation of SQUID magnetometers that measure the full magnetic field tensor.

You can analyse the model components, the vertical gradient or full tensor. The 3D visualisation assists with understanding the relationship between the model and the tensor direction. The 3D colour modulated ribbon allows you to colour code the ribbon by another channel such as terrain clearance.

Mapping & Imaging

ModelVision supports a variety of mapping methods and allows you to superimpose the plan view of your model in the map view.

Processing & Utilities

ModelVision is packed with useful utilities such as minimum curvature gridding, grid filtering, line filtering and a calculator that operates on lines, points, drill holes and grids.

The utilities include a survey simulator and a drillhole simulator that can be tagged to a topographic surface and viewed in 3D.

ModelVision is integrated with other products and extensions designed to optimise the benefits derived from advanced interpretation of magnetic and gravity data.

Optional Features

Encom AutoMag

AutoMag is an advanced implementation of Dr Zhiqun Shi's Naudy method for automatic location and inversion of magnetic anomalies. It is integrated with ModelVision to provide confirmation of automated solutions in a way that cannot be achieved by conventional automated methods.

Any solution from AutoMag can be converted to a ModelVision model body and the forward model response compared with the original data.

A suite of QC tools allow you to prioritise the responses, apply strike corrections and use inversion to refine the initial models. The tools are used to obtain rapid estimation of depth of cover for petroleum, mineral and groundwater applications.
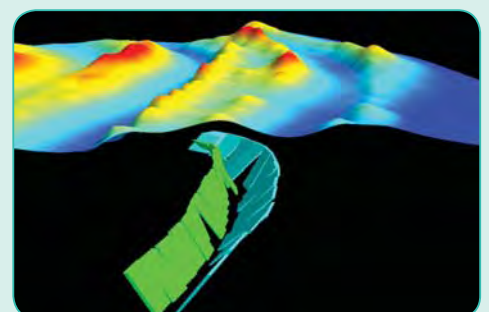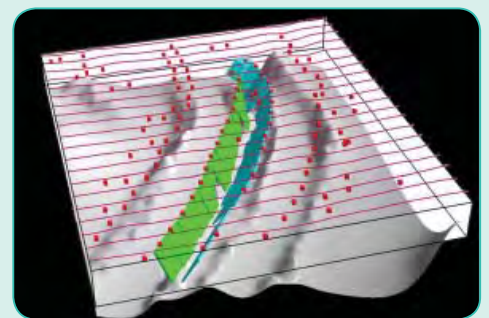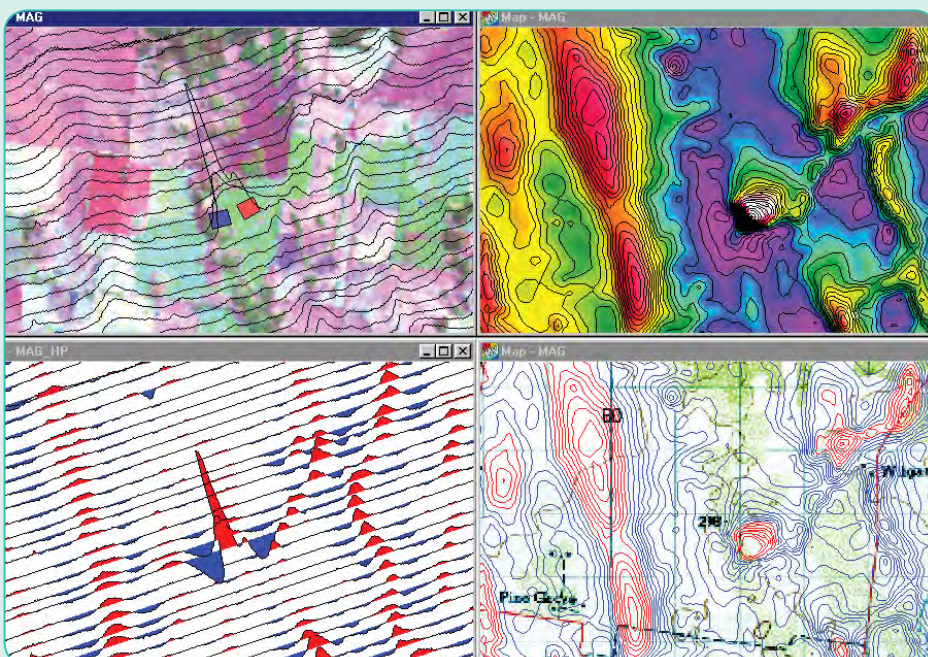
encom⁺ modelvision

UBC-GIF Voxel Models

Encom has developed an optional extension for ModelVision that makes it easy to prepare and run UBC-GIF, GRAV3D and MAG3D smooth inversions.

Use ModelVision to generate the initial model for the inversion along with the associated data and constraint files. The solid models in ModelVision are converted to mesh models by assigning properties to each mesh cell that falls inside a body. The density and susceptibility of that body are assigned to each cell.

You can use the standad UBC tools to visualise the results of the smooth inversion or Profile Analyst's rich range of visualisation options to integrate the inversion results with other models and data sets.

The benefits of using ModelVision with the UBC-GIF programs include:

- Easy connection to industry data formats

- Prepares topographic model

- Prepares data files

- Removal of the regional field

- Prepares a starting model

- Prepares a bounds file property

- Runs the UBC-GIF programs

- Visualise the results with UBC viewer

- Visualise the model in Profile Analyst

ModelVision allows you to integrate geological controls into the UBC-GIF smooth inversion. ModelVision can create and populate the entire model with physical properties based on geological modelling with limited controls.

You can add an unconformity layer to minimise the leakage of high density or susceptibility values into a low contrast domain. This forces the properties to be distributed below the unconformity and subsequently produces more realistic geological solutions.

A comparison of the ModelVision model and UBC Inversion results in Profile Analyst allows you to assign confidence zones to the UBC inversion.

Encom can supply all UBC-GIF software.
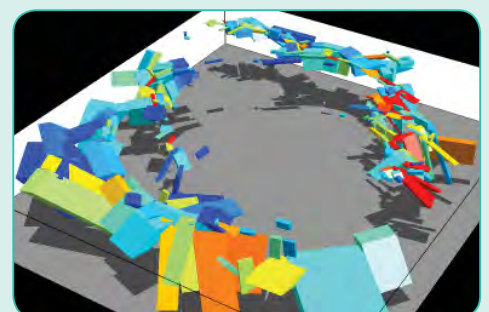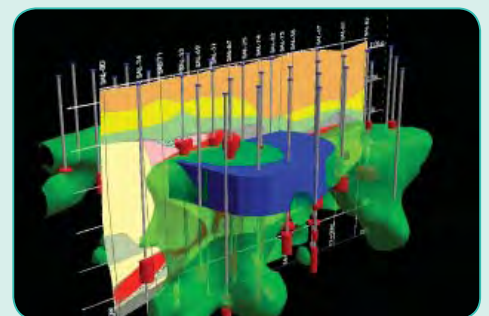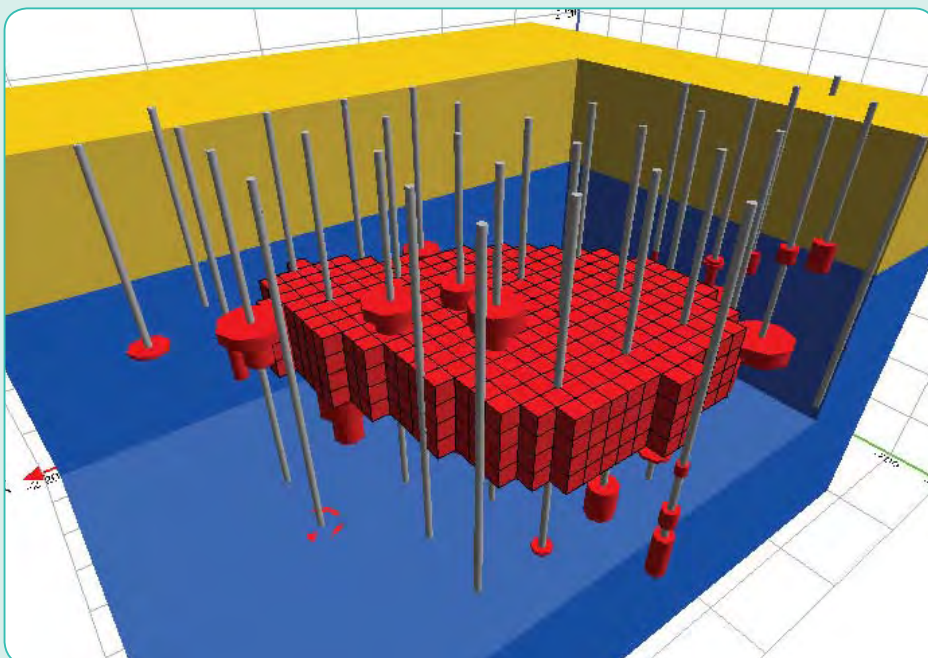
encom modelvision

Related Encom Products

Encom Profile Analyst

Profile Analyst is Encom's premier model and data integration tool for 1D, 2D and 3D geoscience information. It connects to other Encom products and many other industry geoscience products such as Oasis montaj™, Intrepid and ER Mapper. ModelVision provides direct support for the following information types:

- 3D models

- 3D cross-sections

- Model computations for lines, points, drill holes & grids.

- Synthetic drillholes

Use Profile Analyst to compare your results with other information sources such as drillhole data, outcrop mapping, models from other geophysical packages.

Encom QuickMag

QuickMag provides a rapid method of 3D modelling of magnetic targets and can export its models in ModelVision tabular block or polyhedral format.

QuickMag Pro is used to map the distribution of magnetic sources on an unconformity surface. This includes dykes, steeply dipping and folded volcanic units and intrusive plugs.

QuickMag includes an expert system for auto-identification of 2D magnetic anomalies and an advanced inversion technology that allows you to match the inversions for different geological styles.

QuickMag segments a complex geological target into a set of linked tabular blocks whose properties can vary in a controlled manner along the axis of the model.

Use the results from QuickMag to guide your interpretation in ModelVision.

Specifications

Import

ModelVision supports a wide range of industry standard line, point, grid and image data formats.

Lines
- General ASCII import wizard
- ASEG-GDF2
- Geosoft Oasis montaj (.GDB)
- Geosoft multi-line (.XYZ)
- Geosoft single line (.DAT)
- Oasis multi-line (.XYZ)
- Simple XYZ format (.LIN)
- Mutli-file single line (.DAT)
- Separate header and data (.HDR + .LIN)
- ER Mapper 4,5 (.ASC) (.TXT)
- AMIRA (.TEM)
- TOOLKIT (.TK)
- External Data Link (User defined)

Grids
- ER Mapper (.ERS)
- Geosoft uncompressed (.GRD)
- ASEG-GXF
- USGS (.USG)
- Geopak (.GRD)
- Encom (.GRD)

Drillholes
- Geosoft Oasis montaj™ (.GDB)
- Simple XYZ (.LIN)

Points
- Oasis montaj (.GDB)
- Simple XYZ (.PTS)
- Geosoft single Line (.DAT)
- ER Mapper 4 ASCII Profile (>ASC)
- Toolkit format (.TK)
- AutoMag solutions

Images

Images can be imported as Microsoft BMP files and geo-referenced for inclusion in cross-sections or map views. Depth-converted seismic sections or scanned geological sections can be used as backdrops on model sections.

Vectors
- ESRI Shape files (.SHP)
- MapInfo interchange (.MIF)
- AutoCad 2D (.DXF)
- ER Mapper vector (.ERV)

Models
- ModelVision and Toolkit
- (.TKM)Autocad 3D (.DXF)
- External links

Export

You have access to a wide range of export facilities for both models and data created within Modelvision.

Lines
- ASEG-GDF2
- Oasis montaj™ (.GDB)
- Geosoft multi-line (.XYZ)
- Geosoft single line (.DAT)
- Simple XYZ format (.LIN)
- TOOLKIT format (.TK)
- AMIRA format (.TEM)
- External Links (User defined)

Grids
- ER Mapper (.ERS)
- ASEG-GXF
- Geosoft (.GRD)
- USGS (.USG)
- Geopak (.GRD)
- Encom (.GRD)

Drillholes
- Oasis montaj (.GDB)
- Simple XYZ (.LIN)

Points
- Oasis montaj (.GDB)
- Simple XYZ (.PTS)
- AutoMag solutions

Models
- ModelVision (.TKM)
- TOOLKIT (.TK), AutoCAD 3D (.DXF)
- UBC mesh model
- External link (user defined)
- Profile Analyst geocoded sections (.EGB)
- GoCAD (tsurf)

encom modelvision

Encom Profile Analyst

ModelVision provides support for Profile Analyst in a variety of methods including:

- Grid (.ERS)
- Lines (.GDB)
- Holes (.GDB)
- Points (.GDB)
- Models (.3D .DXF)
- Sections (.EGB)
- UBC-GIF voxel model

You can save nearly all data, grids and models in a format that is immediately available for visualisation in Profile Analyst.

Images

Most graphic windows support the creation of high-resolution bitmaps (BMP) as an export option. These images are suitable for inclusion in reports.

Filters

Line Convolution
- Low/high/band pass
- 1st/2nd horizontal derivative
- 1st vertical derivative
- Analytic signal
- Moving average
- Median
- Fourth difference
- Upward continuation
- AGC
- Noise generator

Line FFT
- Low/high/band pass
- 1st horizontal derivative
- 1st vertical derivative
- Upward/downward continuation
- Reduction to the pole
- Pseudo-gravity
- Band limited noise genertor

Grid Convolution Filters
- Average
- Gaussian
- Low/high/band pass
- Laplace
- Sharpen
- Sobel
- Illumination
- Noise generator

FFT Grid Filters

The research capabilities of ModelVision Pro have been extended with the introduction of a comprehensive range of 2D FFT filters that include the following:

- Low/high/band pass
- x, y, z component transforms
- Upward/downward continuation
- 1st, 2nd vertical derivative
- fractional derivatives
- x, y horizontal derivatives
- reduction to equator
- reduction to pole
- pseudo-gravity transform
- pseudo-magnetic transform

Model Types
ModelVision models are designed to provide convenient methods for creating and editing a range of simple to complex geological shapes.

- Polygonal vertical cross-section with dip
- Polygonal horizontal cross-section
  > dip
  > azimuth
- Inclined upper surface
- Frustum
- Dipping tabular block
- Ellipsoid
- Sphere
- Horizontal elliptic cylinder

Combinations of these basic building blocks can reproduce almost any geological environment.

Inversion Methods
The guided inversion method allows you to free parameters from one or more bodies at a time. Parameter ranges can also be fixed to ensure that they do not move outside reasonable bounds.

Modelling Methods

Section (3D)

Create, select and edit models in a single section or multiple geological sections with all the advantages of 2D modelling in a 3D volume. Graphical access to body-specific spatial attributes such as polygon vertices or body location.

Map (3D)

Create, select and edit models in a map view. Graphical access to body specific spatial attributes such as polygon vertices or body location. Use the body property to access spatial, physical property and visual attributes.

Field Components

Gravity modelling supports the total gravitation attraction Gx, Gy, Gz and the full gravity tensor Gzz, Gxx, Gyy, Gxy, Gxz, Gyz and some derived components such as the analytic signal.

Magnetic modelling supports the total magnetic intensity Bx, By, Bz and along-line components and the full magnetic tensor. The along-line component can be used for the axial drillhole component.

Active Data Zones

ModelVision can work with a complete survey by activating segments of the survey for modelling. This may be a single line, multiple lines or segments of one or more lines. In this way, it is possible to reduce the large computational overhead of modelling large data sets by focusing on anomalous data regions.

encom modelvision

Manual/Immediate/Compression

You can model using compute-on-demand or immediate (real-time) computing modes. If you are working with large data sets and complex models, you can speed up the computation process using a data compression option.

In-line Filters

You can turn on an active filter that allows you to view your model and field data through the same filter. Use a first vertical derivative filter to improve depth precision or an upward continuation filter for noise affected data.

Regional 1D/ 2D

Manipulate 1D and 2D regional gravity and magnetic fields depending upon the modelling mode. Auto-compute a starting regional and then use manual editing methods to adjust the shape.

3D Visualisation

- Models
- Flight path/profiles
- Drillholes
- Points
- 3D Grids with colour drape
- AutoMag points
- Vectors

Map Visualisation

- Model
- Stacked profiles
- Contours
- Grid profiles
- Vector files
- Drill holes
- Images
- Bitmaps
- Points/symbols
- AutoMag solutions
- Profile vectors
- Base lines
- Flight path
- Legend
- North arrow
- Coordinate grid

Section Visualisation

- Model (colour modulation)
- Gravity and magnetic data
- Computed magnetic and gravity data
- Regional gravity and magnetic field
- In-line filters
- Auxiliary curves
- Vectors
- Terrain
- Data collection path
- Drillholes
- AutoMag solutions
- Similarity coefficients
- Bitmap sections (geocoded)
- Titles and legends
- Next line function

Utilities

- Line and grid calculator
- Line interpolation
- Synthetic survey generator
- Synthetic drillhole generator
- Synthetic grid generator
- Minimum curvature gridding
- Sample grid to lines
- Statistics
- Data maintenance
- IGRF values for anywhere in the world
- IGRF grid generator

System Requirements

ModelVision runs on Microsoft Windows 98, NT, 2000 and XP. The amount of memory required is operating system dependent. 256MB of RAM is recommended, but ModelVision will run with 128MB on most versions of the operating system.

Contact Encom

Sydney
Level 1/123 Walker Street
North Sydney NSW 2060 Australia
T +61 2 9957 4117 F +61 2 9922 6141

Melbourne
Level 1/469 Glenhuntly Road
Elsternwick VIC 3185 Australia
T +61 3 9523 0033 F +61 3 9523 2296

Perth
Level 2/1050 Hay Street
West Perth WA 6005 Australia
T +61 8 9226 0101 F +61 8 9226 0102

London
59-60 Thames Street, Windsor
Berkshire SL4 1TX United Kingdom
T +44 1753 272332 F +44 1753 272334

info@encom.com.au
www.encom.com.au

encom advanced realities

Encom QuickMag 2.0

New version now available

- Important release containing significant enhancements requested by QuickMag users

- Available to users with current subscriptions to Encom's Standard Support and Updates service

- CD distribution for currently maintained licences

- Also available for download from the Encom website

CD Upgrade

A CD upgrade will be automatically shipped to all QuickMag licensees with current Support and Updates service subscriptions.

Website Download Instructions

Version 2.0 is also available for download from the Encom website. The Encom website is located at **www.encom.com.au** and the Downloads option is at the bottom of the home page. From here, select Encom QuickMag 2.0. The file size is approximately 26Mb.

Enhancements

Encom QuickMag 2.0 has many new features and improvements based on recommendations from our clients and our own testing.

1. A new image engine allows you to overlay interpretation models on images other than magnetic images. You can display aerial photos, scanned basemaps, satellite imagery etc using Geotiff or ER Mapper image formats.

2. You can now create a starting model as an alternative to auto-detection by drawing a polygon around the anomaly. This can be used in noisy environments where the auto-detection fails to derive a suitable model.

3. The area used in inversion (called the inversion area) is selected automatically, but can now be edited to remove unwanted noise or interference.

4. Most operations are now available from a one-click toolbar button.

5. Added depth extent assignment. This allows modelling of sills and shallow depth extent geology. QuickMag operates effectively on infinite depth extent problems but limiting the depth extent makes these problems more realistic. Examples include diatremes, drainage anomalies and sills.

6. Low field inclination (< 30 deg) is now supported. Manually creating the starting model also works well with this new feature.

7. Create synthetic model grids for a general dipping prismatic body at any IGRF setting and then test the results in QuickMag. This can be used to document what a magnetic anomaly will look like anywhere in the world. This is also a useful teaching tool.

8. Support for an associated digital terrain grid where the model's area is adjusted to the elevation at the centre of the body. This allows correct visualisation in Profile Analyst 3D.

9. Export of TKM files to ModelVision Pro with support for the plunging prism model or the multi-block models. This allows refinement of the models in ModelVision Pro without having to build the model manually.

10. New help system with guides providing assistance when internal processes fail to achieve a suitable goal and generate an error message.

11. Enhanced model and text file export of individual or all model results.

12. Interactive expert setting to allow access to advanced features for changes to templates and dynamic adjustment of the dialogs to reduce complexity during normal operations.

13. Arbitrary traverses allow you to quickly test the model precision in any direction not covered by the standard cross-sections.

14. Create faults independently from the model so that they can be picked up automatically when a fault option is selected for inversion.

15. Edit fault, dragline and body shapes for model refinement purposes.

Note: The changes in QuickMag 2.0 are so extensive that we cannot support sessions for Release 1 in Release 2. Users should retain their existing 1.0/1.1 licence if they have projects that are active.
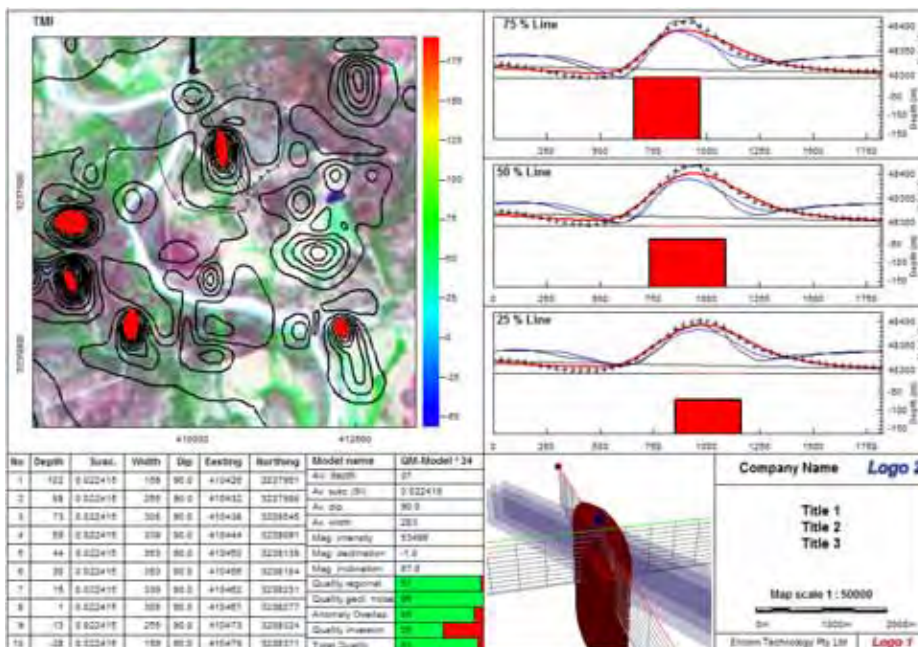
For more information, contact Encom Technology in Sydney.

Head Office

Level 2, 118 Alfred St
Milsons Point
NSW 2061, Australia
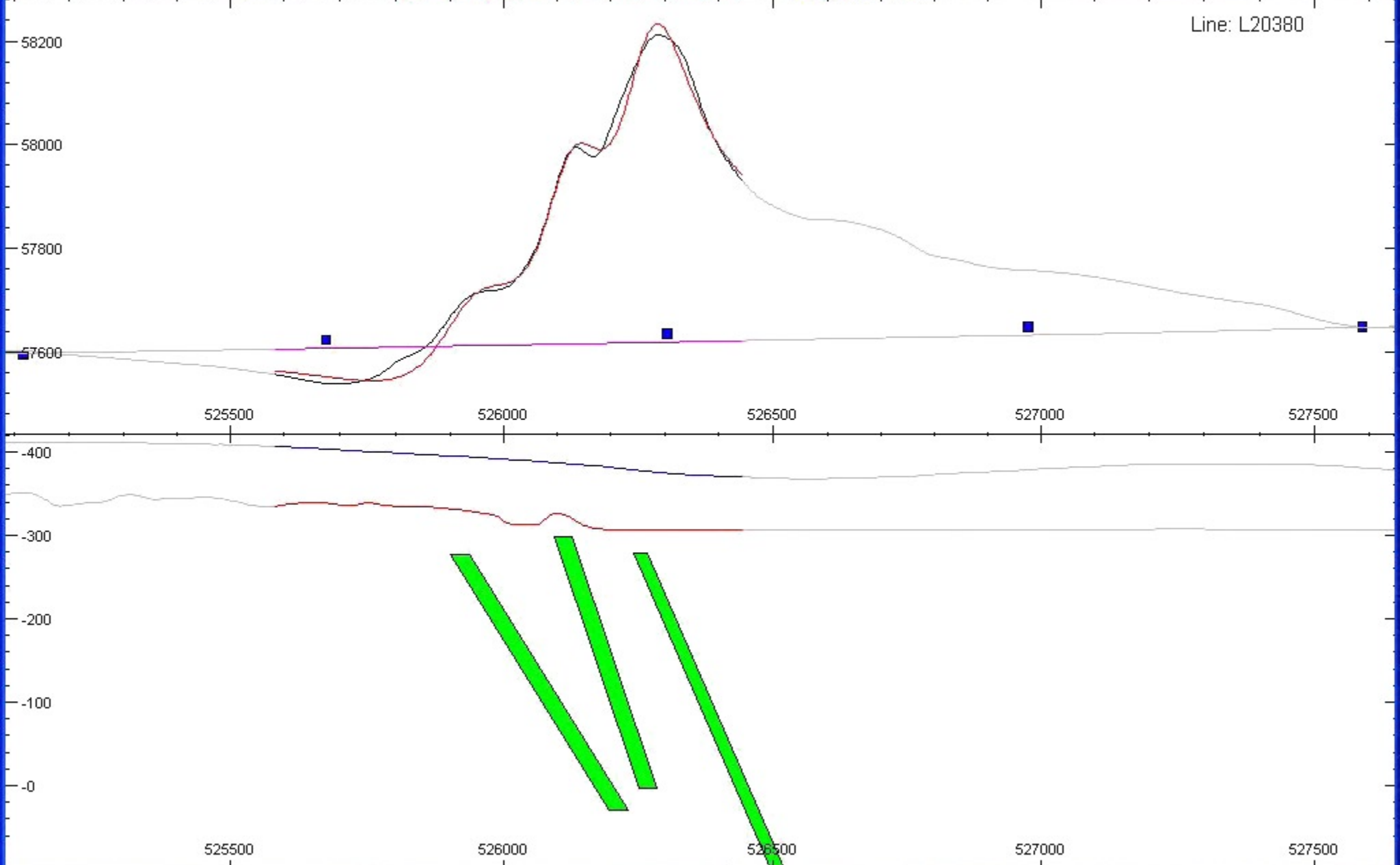Tel +61 2 9957 4117
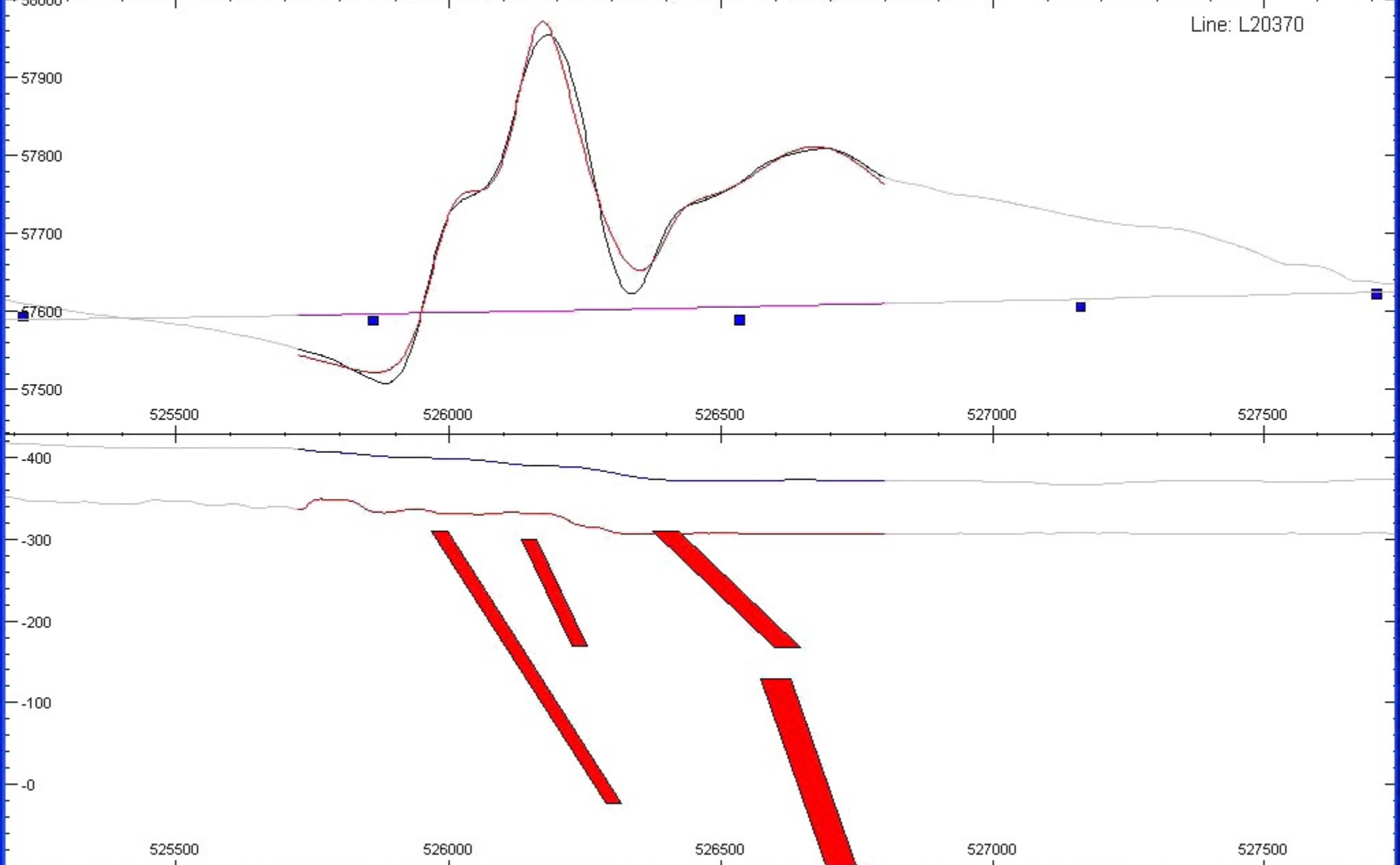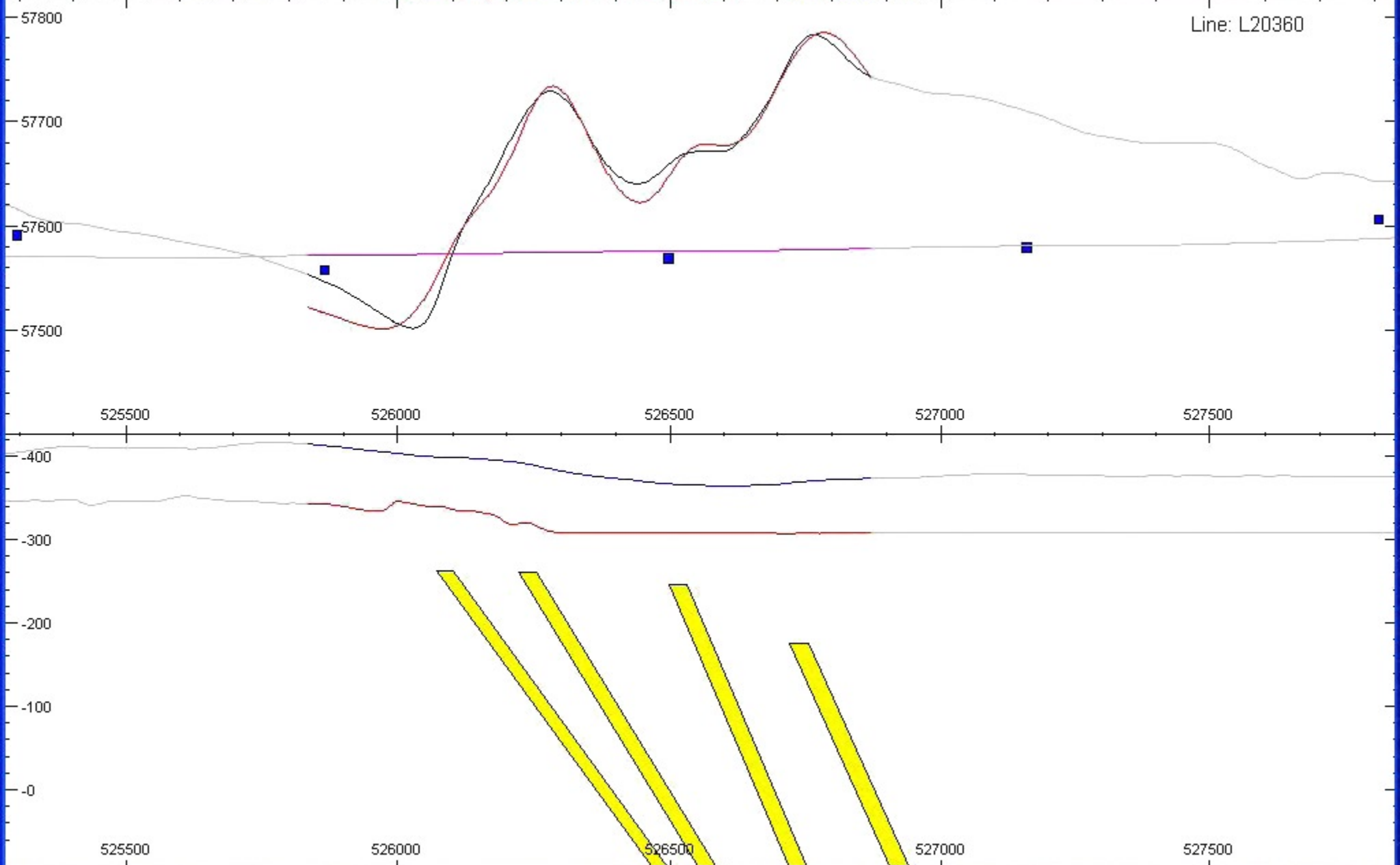Fax +61 2 9922 6141

World Wide Web
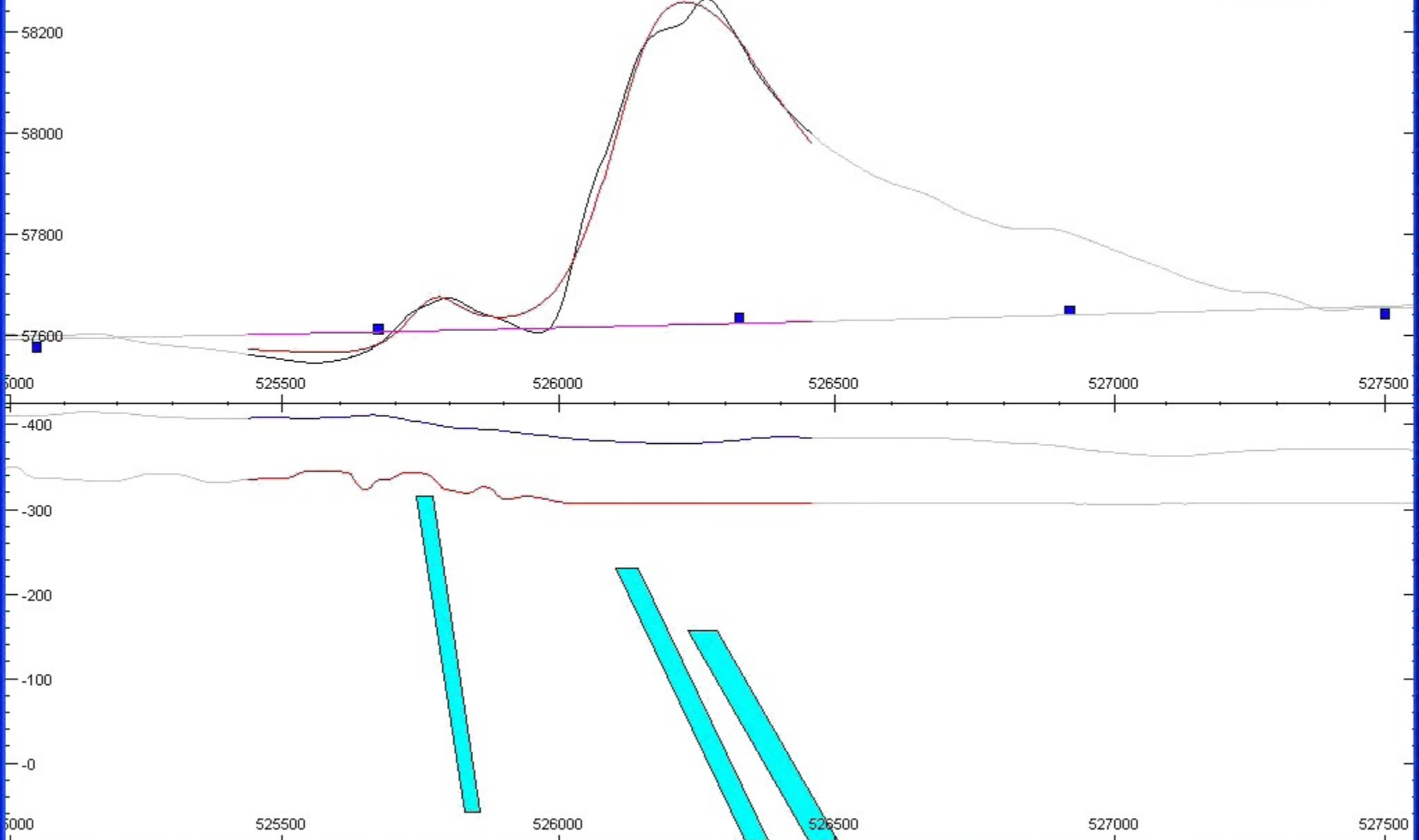
www.encom.com.au

Email

info@encom.com.au

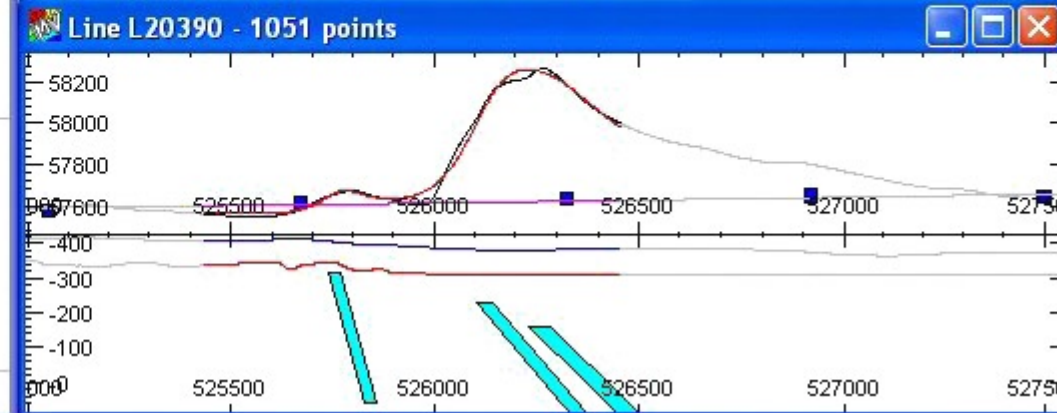# APPENDIX F ARCHIVE DVD